Kraus Johann (Orcid ID: 0000-0002-9534-6295)
Kestler Hans (Orcid ID: 0000-0002-4759-5254)
Schön Michael (Orcid ID: 0000-0002-8905-1810)

Title page

The Journal of Comparative Neurology
Research in Systems Neuroscience
DOI 10.1002/cne.25233

RESEARCH ARTICLE

Funding

This work was made possible by funding from the Hans & Ilse Breuer Foundation, Frankfurt am Main, Germany (HB), and supported by funding from the DZNE, Ulm site (TMB). This work received funding from the European Union's Horizon 2020 Research and Innovation Programme, grant agreement No. 785907 (HBP SGA2) and No. 945539 (HBP SGA3) (KA).

Conflict of interest disclosure

We hereby declare to have no current or potential conflicts of interest.

Ethics approval statement

The ethics committee of Ulm University approved the study on the lissencephaly cases under the license number 333/16 (Table 2, cases 1 and 2). The brain of a 15-year-old female from the Ulm University tissue archive served as a control (Table 2, case 3). The brain of a 1-day-old male (see Discussion section) also originated from the tissue archive at the Ulm University. Informed written consent for autopsy and for study purposes was obtained previously from the patient's next of kin in compliance with university ethics committee guidelines and German state law governing human tissue usage.

Availability of data

The data that support the findings and are not already included in figures or tables of this study are available from the corresponding author upon reasonable request.

Received: May 20, 2020; Revised: Aug 08, 2021; Accepted: Aug 12, 2021

A comparative study of pre-alpha islands in the entorhinal cortex from selected primates and in lissencephaly

Pre-alpha islands in primates and lissencephaly (running title)

Schön M[1], Nosanova A[1], Jacob C[1], Kraus JM[2], Kestler HAK[2], Mayer B[3], Feldengut S[4], Amunts K[5,6], Del Tredici K[4], Boeckers TM[1,7], Braak H[4]

[1]Institute for Anatomy and Cell Biology, Ulm University, Ulm, Germany

[2]Institute of Medical Systems Biology, Ulm University, Ulm, Germany

[3]Institute of Epidemiology and Medical Biometry, Ulm University, Ulm, Germany

[4]Clinical Neuroanatomy, Department of Neurology, Center for Clinical Research, Ulm University, Ulm, Germany

[5]Institute of Neuroscience and Medicine (INM-1), Research Center Jülich, Jülich, Germany

[6]C. and O. Vogt Institute for Brain Research, University Hospital Düsseldorf, Heinrich Heine University Düsseldorf, Düsseldorf, Germany

[7]DZNE, Ulm site, Ulm, Germany

Correspondence to: Tobias M. Boeckers, tobias.boeckers@uni-ulm.de; Michael Schön, michael.schoen@uni-ulm.de

Contributions

The study design was generated by HB, KDT, KA, TMB, and MS. Analyses were conducted by AN, CJ, SF, and MS. KA provided access to the Zilles, Amunts (Stephan) mammals'

collections and contributed to the analysis. AN, HK, JK, and BM contributed to the statistical calculations. Writing of preliminary and final versions of the manuscript was the joint work of all authors.

Acknowledgments

We want to thank the NIH brain bank for kindly providing tissue from individuals with lissencephaly. We thank René Hübbers and Ulrich Opfermann-Emmerich for capable assistance in providing and acquiring the primate brain sections. The authors thank Mr. David Ewert (Ulm University) for skillful assistance with the figures (black and white image editing).

In memoriam Karl Zilles († 26.04.2020)

Abstract

The entorhinal cortex (EC) is the main interface between the sensory association areas of the neocortex and the hippocampus. It is crucial for the evaluation and processing of sensory data for long-term memory consolidation, and shows damage in many brain diseases, e.g., neurodegenerative diseases, such as Alzheimer's disease and developmental disorders.

The pre-alpha layer of the EC in humans (layer II) displays a remarkable distribution of neurons in islands. These cellular islands give rise to a portion of the perforant path – the major reciprocal data stream for neocortical information into the hippocampal formation. However, the functional relevance of the morphological appearance of the pre-alpha layer in cellular islands and the precise timing of their initial appearance during primate evolution are largely unknown. Here, we conducted a comparative study of the EC from 38 non-human primates and *Homo sapiens* and found a strong relationship between gyrification index (GI)

and the presence of the pre-alpha cellular islands. The formation of cellular islands also correlated wih brain and body weight as well as neopallial volume. In the two human lissencephalic cases, the cellular islands in the pre-alpha layer were lacking. These findings emphasize the relationship between cortical folding and island formation in the entorhinal cortex from an evolutionary perspective, and suggest a role in the pathomechanism of developmental brain disorders.

Keywords: entorhinal cortex, gyrification, cytoarchitecture, pre-alpha islands, lissencephaly, phylogeny

Introduction

The human entorhinal cortex (EC) is a cortical region at the rostromedial side of the temporal lobe extending over the ambient gyrus and the rostral portions of the parahippocampal gyrus. It is part of the allocortex. Ramón y Cajal coined a still valid definition of the EC as the part of the mediobasal temporal cortex, which gives rise to a neuronal link to the hippocampus known as the perforant path (Cajal, 1902). He realized that the EC represents the major input-output station for data transfer between the neocortex and the hippocampus (Braak & Braak, 1992; Braak, Del Tredici, Bohl, Bratzke, & Braak, 2000; Canto, Wouterlood, & Witter, 2008). The EC integrates sensory information for memory and learning as well as conscious integration of external in- and output. It is involved in brain diseases, including temporal lobe epilepsy, Down's syndrome, schizophrenia, Rett syndrome, Huntington's disease, progressive supranuclear palsy, argyrophilic grain disease, Parkinson's disease, dementia, and Alzheimer's disease (Braak & Braak 1992; Hof et al. 1995; Mann & Esiri 1989; Braak & Del Tredici 2015; Braak & Braak 1990; Leontovich et al. 1999; Wakabayashi, Honer, Masliah 1994; Braak et al.

2000; Kuhn et al. 2018). In Alzheimer's disease (AD), for example, the presence of intraneuronal tau pathology within projection neurons of the cellular islands of layer pre-alpha gradually causes extensive disruption of efferences to the hippocampus (Heiko Braak, Braak, Yilmazer, & Bohl, 1996), such that, in late-stage AD, the hippocampal formation becomes 'disconnected' from the neocortex (Delbeuck, Collette, & Linden, 2007; Hyman, Van Hoesen, Kromer, & Damasio, 1986; Kemper, 1984; Reid & Evans, 2013; Van Hoesen & Hyman, 1990).

Cytoarchitectonically, a cell-poor lamina dissecans separates an external principal layer (pre) from the internal principal stratum (pri). The cortical layers have been differently numbered and named. Lorente de Nó defined six layers with Roman numerals. Layer II neurons are arranged in clusters – mostly designated as islands – with an almost neuron-free interspace containing the neuropil. With Nissl staining, two inner and two outer strata separated by the lamina dissecans, are discernible. To avoid confusion with neocortical layers, other authors refer to the allocortical entorhinal layer II as layer pre-alpha as it was termed by Rose (Braak & Braak, 1992; De Nó, 1933; Insausti, 1993; Insausti, Muñoz-López, Insausti, & Artacho-Pérula, 2017; Rose, 1927). We mostly follow this designation as well. Several features, e.g., different immunoreactive neurons in the layers, neurons in patches as in pre-alpha layer, and the corresponding interneuron cytoarchitecture, hint at a module architecture of the pre-alpha islands (Solodkin & Van Hoesen 1996), whose intrinsic and extrinsic connections are well known, although the transition to function remains elusive. The cellular islands give rise to a portion of the perforant path – the major reciprocal data stream for neocortical information into the hippocampus, and are therefore key in processes of learning and memory, and its disturbances, e.g., in AD (Canto, Wouterlood, & Witter, 2008).

The EC receives input from many association areas, including prefrontal areas. We hypothesized that there might be an impact of increased size of the neocortex, measured as the

gyrification index, neopallial volume, and partly also in brain weight, on the existence of pre-alpha islands in different species and in a pathological condition of cortical folding.

Therefore, we examined the brains of 38 non-human primates and two human individuals for the presence or absence of pre-alpha islands in relationship to the gyrification index (and other measures for neopallial increase) to test the hypothesis of a relationship between the expansion of the cortex in evoluation and pre-alpha island formation. Secondly, we studied cellular islands in two casese of lissencephaly, i.e an abnormal formation of cerebral gyri during ontogeny (Donato et al., 2017) in comparison to normal development.

Materials and Methods

Tissue

Animal brains: Cresyl violet/Nissl-stained tissue sections from the brains of 39 primates including *Homo sapiens* were analyzed: 18 Strepsirhini, two Haplorhini (Tarsiiformes), eight Haplorhini (Semiformes/Platyrrhini), and eleven Haplorhini (Semiformes/Catarrhini) (listed in Table 1; Figures 1-3). Sections are part of the collection of the Cecile and Oskar Vogt Institute for Brain Research of the Heinrich Heine University of Düsseldorf.

Human brains: Two cases of lissencephaly were obtained from the NIH Neurobiobank at the University of Maryland, Baltimore, MD (cases 683, 4524) (Federeal Wide Assurance: FWA00025179). Demographic and neuropathological data for NIH cases 683 (case 1) and 4524 (case 2) are provided in Table 2. The brain of a 15-year-old female from the Ulm University brain bank served as a control (Table 2, case 3).

Methods

Analysis of histological, coronal sections of non-human primate species and humans

In most instances, two individuals from each species were examined, if available one male and one female. Human individuals were a male (39 years of age) and female (43 years of age). Respresentative images are shown from one individual per species in Figure 1. The brain collections includes coronal section series that permitted assessment of the EC over the entire rostro-caudal extent. The quality and intensity of the staining were, in part, very different. The investigator (MS) was blinded to the parameters on the animals (e.g., GI, brain weight, etc.) at the time of examination to avoid biased assessment. Multiple coronal sections of both hemisphers were examined at four rostro-caudal positions (locations L1-L4): L1 was located at the level of the maximal extent of the amygdala, L2 at the most rostral appearance of the stratum granulare (dentate gyrus), L3 at the most rostral distinct medio-lateral extent of the stratum granulare, and L4 was located at the most caudal position where the hippocampus rises supracommissurally or just before the disappearance of the lamina dissecans. One individual from each species was reexamined in a second sitting to corroborate the categorization of cellular island formation.

Pre-alpha islands were classified into three categories considering their appearance between L1 and L4: (1) n = no cellular islands, i.e., the cellular band was continuous; (2) b = between, the pre-alpha layer was wavy or implied interrupted; (3) y = yes, islands were clearly visible. A summary category was then generated: if there were only n at all four positions, it was classified as ‘n’, if there were only y, then ‘yyy’. If there was one b or y, then ‘b’ or ‘y’, if there were at least two b or y and if one of them was at L3, ‘bb’ or ‘yy’.

In *Pongo pygmaeus*, L1 was classified as b. However, because the amygdala area was artifactual, acquisitions were made between L1 and L2 - here islands are clearly visible. It was also difficult to distinguish between ‘b’ and ‘y’ at L1.

Acquisition and processing of the images

Images were acquired using Zeiss Axio Observer with an isotropic point resolution of 4.09 µm/pixel. Sections were oriented so that left is medial (see Figure 1). Artefacts (air bubbles, dust particles) in the empty areas surrounding the tissue sections and, to a very limited extent, in the sections were carefully removed without topographical/anatomical relationships especially of the pre-alpha layer (also in the images from tissue described in the following paragraph). Minor adjustments were made for brightness and contrast.

Tissue processing of human lissencephalic and control tissue

Coronal blocks were cut with a vibratome (Leica Biosystems) at a thickness of 100 µm. A single free-floating section from each case was pretreated with performic acid and stained with aldehyde fuchsine (12763.00500, Morphisto, Frankfurt am Main, Germany) for selective staining of lipofuscin deposits combined with a basophilic Nissl stain (Darrow red; 211885, Sigma-Aldrich, Steinheim, Germany) for topographical overview and to mark neuronal loss, as described previously (Braak 1984; Braak & Braak 1991). Tissue sections were cleared, mounted, and cover-slipped (Histomount, National Diagnostics, Atlanta, GA, USA). Image acquisition was performed with an Olympus BX61 microscope (Olympus Optical, Tokyo, Japan). Digital micrographs were taken with an Olympus XC50 camera using the Cell D® Imaging Software (Olympus, Münster, Germany). We used small coronal blocks available and cannot draw conclusions over the whole rostro-caudal EC extent.

Statistical analysis of categorization with continuous data

Continuous brain data (GI, brain weight, neopallial volume, body weight, and ratios neopallial volume-to-brain weight, brain weight-to-body weight) as obtained from the publication of Zilles and colleagues (Zilles et al., 1989) were compared with the categorization defined by presence or absence of cellular islands in the pre-alpha layer from this present study

(Figure 3). Data were averaged for multiple individuals of a species (Table 1 in Zilles et al., 1989), and these mean values were used for further analyses.

The correlations between the island formation score and all six continuous parameters were calculated in the statistical computing software R v.4.0.5. To account for possible dependencies in the primate data, we used a computer-intensive test procedure that exhaustively evaluates all possible correlations (Spearman's rank correlation) in all subsets of sample size two to six of all island formation categories, in total 4,598,438.

We additionally investigated a relationship between the island formation and the continuous brain morphological parameters by using the Bayesian generalized linear mixed models with the ordinal phenotype distribution (probit link). The phylogenetic dependency was introduced into the models as a random effect. We used an inverse gamma prior for random effects and ran each analysis for 5,000,000 interactions with burn-in of 1,000 and the thinning interval equal to 500. The pMCMC (Bayesian p) value, a posterior probability that the effect parameter is different from zero, was used to determine the significance of the parameter estimates (statistically significant if pMCMC < 0.05). The analysis was performed by implementing functions from the 'MCMCglmm' R package (Hadfield, 2010). GI was squared because an increase in gyrification leads to an increase in (2-dimensional) cortex surface area. Levels of significance were defined as $p<0.05$ = *, $p<0.01$ = **, and $p<0.001$ = ***. Brain weight, body weight, and neopallial volume values were log transformed prior to the analysis to reduce the skewness of the data.

Since we used the phylogenetic tree with divergence times to account for the phylogenetic autocorrelation in the 'MCMCglmm' model, we had to exclude *Galagoides demidoff* species from statistical analysis. These two individuals had very different island characteristics (Table 1, S14 and S15). By including only one species, we would introduce bias

into our model. Yet if both primates were present in the paradigm, this would lead to false pedigree construction and generate further computational errors.

Ancestral character state reconstruction

The likelihood that a common ancestor possessed the feature 'cellular islands' in the entorhinal cortex was calculated (see Figure 4). The phylogenetic tree was established using the open-access TimeLife database (Hedges, Marin, Suleski, Paymer & Kumar, 2015; Kumar, Stecher, Suleski & Hedges, 2017). In order to estimate the ancestral state reconstruction we applied function ace for discrete characters from the 'ape' R package (Paradis & Schliep, 2018) to the phylogenetic tree and the states of the island formation. The resulting reconstruction was built by fitting the equal-rates model for the maximum likelihood estimation with the joint reconstruction (Pagel, 1994). The final tree was plotted using functions built in 'ape' and 'phytools' (Revell, 2011) R packages. The length of the tree edges corresponds to the divergence time estimates between the species (Hedges, Marin, Suleski, Paymer & Kumar, 2015, see Figure 4). Also here *Galagoides demidoff* was excluded.

Results

Pre-alpha cellular islands in primate brains

Figure 1 shows examples of 39 species. On pages 1 and 2, 18 Strepsirrhini are displayed. Note that S14 and S15 are from two individuals of the same species (*Galagoides demidoff*). Whereas the male had islands in pre-alpha, they were completely absent in the female. However, the island expression in the other species was largely identical between the two individuals examined. The images shown in Figure 1 correspond to position L3 (see also Table 1).

From rostral to caudal, four positions were chosen that were comparably detectable in all species. As an example, from seven species, these four rostrocaudal positions are shown with the hippocampus, including the four Hominidae (Figure 2).

To establish relationships between continuous parameters that were known from a previous publication (Zilles et al., 1989), such as gyrification and other parameters, and the presence of pre-alpha cellular islands in the primates studied, we analyzed the different species in a comparative approach including non-human and human primate brains (Figure 3). The available species ranged from those with smooth cortical surface = lissencephalic animals (e.g., *Saguinus oedipus*, *Loris tardigradus)* to those with a complex gyrification, with *Homo sapiens* having the highest gyrification index. While most species of the Strepsirrhini, Platyrrhini, and Tarsiiformes did not have distinct islands ('n', 'b', or 'bb'), almost all Catarrhini had them in the pre-alpha layer of the EC. When looking at the cellular island formation at the individual positions, a rostro-caudal gradient with decreasing expression is noticeable for all species (Table 1).

In particular beginning from ‘y’ a relationship with increase of these parameters becomes apparent except brain weight-to-body weight ratio. Gyrification index and neopallial volume both showed a significant positive correlation with the proposed island formation score ($p<2e-16$***), while brain weight-to-body weight ratio showed a significant negative correlation ($p<2e-16$***, sign test). The determined median correlation of the parameters were as follows: GI 0.58, neopallial volume 0.63, brain weight 0.64, body weight 0.64, neopallial volume-to-brain weight 0.44, and brain weight-to-body weight -0.35. In a second calculation, we added phylogenetic relatedness as another influencing factor. While neopallial volume-to-brain weight and brain-to-body weight were not significant (Bayesian p 0.504 and 0.511), progressive body weight (0.0028**), neopallial volume (0.0018**), brain weight (0.001**), GI (0,002**), and GI^2 (0.0004***) were significant.

We also performed an ancestral character state reconstruction (Figure 4). The Strepsirrhini mainly showed the feature 'b' and with increased likelihood also the common ancestors. Some close relatives, such as S3 (*Eulemur mongoz*) and S4 (*Eulemur albifrons*), had quite similar pre-alpha traits ('bb'), similarly S13 (*Galago senegalensis*) and S16 (*Otolemur crassicaudatus*), or S17 (*Nycticebus coucang*) and S18 (*Loris tardigradus*) as well as their ancestors each seem to have formed similar expressions of the pre-alpha islands ('y' versus 'b'). However, there were also examples of close relationship but distinct island formation, such as between C1 (*Pygathrix nemaeus*) and (*Piliocolobus badius*). S12 (*Daubentonia madagascariensis*) was especially striking: It was the only member of the Strepsirrhini to exhibit islands in more than one of the four rostro-caudal positions of the EC. In contrast to the common ancestor of the Strepsirrhini, the common ancestor of Platyrrhini and Catarrini was more likely to display stronger island formation. While island forming was more prevalent in the analyzed Catarrhini, it was less pronounced in the Platyrrhini. The parvorder Platyrrhini tended to have 'b', 'bb', or 'y', whereas all Catarrhini had 'y', 'yy', or 'yyy'. Only one species, C1 (*Pygathrix nemaeus*), harbored no clear islands in pre-alpha throughout the EC. The common ancestor of C1 to C6 seemed even more likely to have had a lower defined island expression than the common ancestor of C7 to C11, including the Hominidae. In the remainder of the Catarrhini group, only the phylogenetically more distant C7 had a less well-defined island formation, whereas the Hominidae or great apes C8-C11 displayed particularly conspicuous and rostrocaudally continuous islands in the pre-alpha layer.

Pre-alpha islands in the human brains

The two lissencephaly brains revealed a different degree of lissencephaly (see Table 2), and the pre-alpha cellular islands were absent in both. Figure 5 (a) shows a coronal section of the brain of an 8-year-old lissencephalic male (case 1). The pre-alpha layer revealed no clustering of islands (Figure 5 (b)). The same finding was seen in the EC of a lissencephalic

13-year-old male (case 2; Figure 5 (c)). For comparison with an adolescent control, the EC of a 15-year-old female is depicted in Figure 5 (d), where the islands are clearly present in the pre-alpha layer.

Discussion

This study is the first to comprehensively examine the pre-alpha layer in a larger number of primates for the morphological feature of cellular island formation. We showed that cellular islands also evolve independently of phylogenetic relatedness and that the tendency toward cell clustering was already present in the common ancestors of all primates. A rostro-caudal gradient with more pronounced cellular compaction rostrally could also be determined. We found significant differences, with islands in pre-alpha of EC particularly related to the increase in gyrification. Lissencephalic brains, even in the pathological case in human individuals, have significantly low formation of compacted neuronal islands in pre-alpha regardless of their phylogenetic relationship.

In the primate lineage, evolving structures of the brain increase in volume except for those serving olfaction (Stephan & Andy 1964, 1969; Stephan et al. 1981). There is a close relationship between increased gyrification and neocortical volume in primates (Zilles et al. 1989). While brain size is more genetically determined, gyrification may be influenced by non-genetic factors, at least in humans (Zilles, Palomero-Gallagher, & Amunts, 2013).

Neocortex expansion relates with cellular islands in pre-alpha

Here, we found that the degree of gyrification, a marker for neocortex expansiveness, and other parameters that most likely correspond to this (neopallial volume, brain weight, neopallial volume-to-brain weight, body weight), in several species representing a spectrum of non-human and human primates significantly correlated with the presence of the pre-alpha

cellular islands. After squaring the GI, which we saw as an essential factor to see the real brain anatomical processes through an increase in cortex surface area, this factor was most significant. The two human lissencephalic cases examined, accordingly, displayed completely island-free pre-alpha layers as we frequently observed in virtually lissencephalic animals. We hypothesized that there might be a connection between the extent of the neocortex and the presence of the pre-alpha cellular islands in layer II of the EC. This idea was driven by other examples, in which cytoarchitectural modules showed a complete overlap with afferently connected non-neuronal structures, e.g., the neuronal grids in the EC representing the external environment (Fyhn et al. 2004) or the somatosensory barrel cortex associated with the whiskers in rodents (Woolsey and Van der Loos 1970). Horton and Hocking, in 1996, described another interesting example of cell segregation in a cortex layer: the ocular dominance columns in layer IV of the area striata of macaques. Newborn monkeys were light-deprived after birth, and it was found that these cell mosaics were already established at birth without visual sensory input (Horton & Hocking, 1996). Also in humans they are already present at birth, as seen in 10 µm thick pigment-Nissl-stained sections from the brain of a 1-day-old male (Supplementary figure). If the EC collects all highly processed sensory data streaming from neocortical association areas toward the hippocampus and beyond (prefrontal neocortex), the cortical representation might be in keeping with topological designation of EC areas (Insausti et al, 1997) and, thus, the cellular islands, to cortical areas and their functions (e.g., in the sense of a 'gyrotopy'). In this line of thought, the increased data stream via the entorhinal region in higher primates and humans might have triggered or exerted an influence on the formation of the cellular islands. It might also explain, in part, the severe cognitive impairment in our lissencephaly cases and in most lissencephalic individuals (Donato et al., 2017). The EC is a 'bottleneck' for mnestic and other higher cognitive functions in humans. Whether the formation of cellular islands is phylogenetically associated with higher cognitive capabilities in primates

can only be speculated. In a very recent work, Piguet and colleagues found different developmental layer- and subdivision-specific patterns of EC development and discuss that this might be owing to distinct neuronal networks of different parts of the EC (Piguet et al., 2020). A conjunctive evolution of the neocortex with the EC is highly likely since the two are massively interlinked by reciprocal connections (Nieuwenhuys, Voogd& van Juijzen, 2007; Schulz & Engelhardt, 2014). The mass of cortical connections increased in various levels of mammalian organization. This main input into the limbic system is phylogenetically and ontogenetically young and expanded enormously from macrosmatic to microsmatic mammals. Along these lines, the lateral and caudal EC, which are most likely the main relays to and from the neocortex, have increased enormously in humans (Insausti 1993). Interestingly, EC neurons appear ontogenetically before neocortical and archicortical ones (Stranahan & Mattson 2010), which might also provide a clue to the key position EC neurons occupy.

The results of correlation calculations between brain-to-body weight measurements were, surprisingly, the only variable that negatively correlated with the formation of islands in pre-alpha in one of the two calculations. Given the positive correlation between brain size and islands, it was anticipated that no correlation would occur, inasmuch as brain size and body weight are generally positively correlated (Finlay, 2009; Shultz, 2010). However, several aspects must be considered: Whereas brain weight is relatively stable within a species and with respect to sex, body weight can vary widely inter-individually, e.g., in obesity. The values we used here for the calculations were predominantly from the few female and male species studied (Zilles et al., 1989) – therefore, biases cannot be ruled out. Sexual dimorphism may also influence both brain and body weight. In particular, mammalian species with small bodies have relatively large brains (Finlay et al., 2009; Shultz, 2010). This is associated with the observation that, for certain basic functions, brain parts are largely independent of body size (Finlay, 2009; Dunbar & Shultz, 2007). When considering the calculations for island formation

with the brain-to-body weight ratio, it is noticeable that some small Platyrrhini species with relatively large brains had few islands. To account for these allometric differences between species, the encephalization quotient was introduced as a better measure to compare brain sizes and cognitive performance between species (Jerison 1973; Shultz, 2010). Furthermore, interpretation of correlation analysis results may not be focused on p-values, since the underlying hypothesis is that r differs from 0. More telling, however, is an assessment of clinical or biological relevance, which suggests only a weak relationship here (r = -0.35).Methodological imitations of the study

In this section, methodological limitations are addressed in greater detail. Although we found a strong correlation between pre-alpha islands and the cortex expansion in various primates species, no direct proof of a direct influence of neocortical surface extent on pre-alpha cellular island formation can be deduced. However and notably, the first appearance of the cellular islands in the thirteenth postovulatory week (Kostović, Petanjek, Judas 1993) is coincident with initial gyrification of the neocortex (White, Su, Schmidt, Kao, & Sapiro, 2010).

Second, it has been described that gyrification is different in the rostro-caudal axis of the forebrain in primates (Zilles et al., 1988). In the present study, the EC was examined at four positions from the amygdala to the caudal end of the hippocampus. This classification allowed for a good anatomical reference between species. Nevertheless, it is unclear whether these anatomical recognition features (e.g., the amygdala or the rostral beginning of the EC) actually have similar cortical connections in all species and are therefore functionally comparable. Whether the EC can in fact be defined as such at all four positions in all species examined is also unclear, inasmuch as it is defined both cytoarchitectonically and by its connections with the hippocampus. Here, the lamina dissecans and neighboring structures, such as the amygdala, cornu ammonis, and dentate gyrus, have been used to distinguish it.

Third, transitions in this study between positions and also the self-defined categories for pre-alpha cell formation are not abrupt but, rather, continuous. Fourth, it has be be acknowledged that the distinction between the three categories (no islands, partially interrupted, distinct islands) was not always sharp; but the intention was to use a semi-quantitative classification. It must be emphasized, however, that the islands are 3-dimensional structures, which were examined in 2-dimensional coronal sections. This may have resulted in an underestimation in some instances.

Fifth, intra-species differences in folding patterns have been described, and the brains analyzed may not fully represent the average of the species (Zilles et al., 2013). Still, we would expect that differences in GI are lower in most of the non-human primates as compared to humans, considering that folding pattern have undergone significant changes during evolution towards humans. Cortical folding in humans is thought to be a result of genetic and non-genetic factors (Schmitt et al., 2020, Fernandez et al., 2016). Mechanical stimuli also play a role (Foubet et al., 2019).

The evolution of pre-alpha islands in primates

Notably, some very closely related species show similar island features in pre-alpha. Brain morphological parameters were rather similar in several closely related species. In other cases, the categories were very similar despite close relationship of the species (C1 and C2). Where these differences originate is largely unclear. According to Zillles et al. (1989), The GI was different in these species (*Pygathrix nemaeus* and *Piliocolobis badius*); thus, this might be – in light of our findings – a major contributing factor. Of interest is S12 (*Daubentonia madagascariensis*), the only representative of Strepsirrhini with clear islands in several rostro-caudal positions. Independent evolution due to low relatedness is likely. The Hominidae (C8-C11) are particularly outstanding: All of them show a distinct island formation in at least three

positions in the rostro-caudal extent of the EC. Their brain morphological parameters (GI, brain weight, neopallial volume) also increased massively.

Most species in our analysis that harbored cellular islands ('y' or higher) belonged to the superfamilies Cercopithecoidea (C1 to C6) and Hominoidea (C7 to C11), also denominated as the parvorder Catarrhini or Old World anthropoids. These groups within the Catarrhini, Cercopithecoidea and Hominoidea, separated approximately 15 million years ago. Both phylogenetic lineages show other common but separately developed features, namely, increased brain volume and decreased olfactory bulb size (Gonzales, Benefit, Mccrossin, & Spoor, 2015). It is possible that, in these two primate groups, the EC islands developed independently owing to the increased brain size and, thus, to the complexity of the cerebral cortex. However, the common ancestor most likely already displayed islands in one region of the EC. While the Hominoidea have cellular islands in pre-alpha in major parts of the EC, they are found in most Cercopithecoidea only in one of the rostro-caudal positions studied here.

Within the major phylogenetic groups of primates (the suborder Strepsirrhini, the infraorder Tarsiiformes, and the parvorders Platyrrhini and Catarrhini), there seem to be two different trends of island formation in pre-alpha. Whereas the ancestors of the Strepsirrhini and Tarsiiformes tended not to have islands ('bb' or lower), they probably were present already in the common ancestor of the Platyrrhini and Catarrhini. The lineages of the parvorders Catarrhini and Platyrrhini separated approximately 50 million years ago (Perez et al., 2013). While only two of the Platyrrhini exhibited islands, most of the Catarrhini did so. This tendency toward more island formation throughout the EC (Catarrhini>Platyrrhini>Strepsirrhini and Tarsiiformes) fits with phylogenetic relationships, on the one hand, and likewise with increasing brain morphological parameters, such as GI, neopallial volume, and brain weight in terms of independent formation of island expression in each of the groups. Therefore, it is likely

that this trait is not simply inherited but is significantly influenced by the increase in neocortex of the different species.

Conclusion

To our knowledge, this is the first study to investigate a possible link between the neocortex increase in primates and pre-alpha island formation. Owing to the strong reciprocal connection of the neocortex with the EC, it stands to reason that cellular islands formed under this evolutionary influence. It could even be that a highly individual pattern of islands is formed, depending on the individual cortical folding in humans, and this, in turn, might have an influence on individual predispositions to neurodevelopmental and neurodegenerative disorders.

References

Braak, H, & Braak, E. (1991). Neuropathological Staging of Alzheimer-Related Changes. *Acta Neuropathologica*, *82*(4), 239–259. https://doi.org/10.1007/bf00308809

Braak, H, & Braak, E. (1992). The human entorhinal cortex: normal morphology and lamina-specific pathology in various diseases. *Neuroscience Research*, *15*(1-2), 6–31. https://doi.org/10.1016/0168-0102(92)90014-4

Braak, H, Del Tredici, K., Bohl, J., Bratzke, H., & Braak, E. (2000). Pathological changes in the parahippocampal region in select non-Alzheimer's dementias. *Annals of the New York Academy of Sciences*, *911*, 221–239. https://doi.org/10.1111/j.1749-6632.2000.tb06729.x

Braak, H., & Braak, E. (1990). Cognitive impairment in Parkinson's disease: Amyloid plagues, neurofibrillary tangles, and neuropil threads in the cerebral cortex. *Journal of Neural Transmission - Parkinson's Disease and Dementia Section*, *2*(1), 45–57. https://doi.org/10.1007/BF02251245

Braak, Heiko. (1984). Architectonics as seen by lipofuscin stains. *Cerebral Cortex. Cellular Components of the Cerebral Cortex*, *1*, 59–104.

Braak, Heiko, Braak, E., Yilmazer, D., & Bohl, J. (1996). Functional Anatomy of Human Hippocampal Formation and Related Structures. *Journal of Child Neurology*, *11*(4), 265–275. https://doi.org/10.1177/088307389601100402

Braak, Heiko, & Del Trecidi, K. (2015). Neuroanatomy and pathology of sporadic Alzheimer's disease. *Advances in Anatomy, Embryology, and Cell Biology*, *215*, 1–162. https://doi.org/10.1007/978-3-319-12679-1

Cajal, S. R. Y. (1902). Sobre un ganglio especial de la corteza esfeno-occipital. *Trabajos Del Laboratorio De Investigaciones Biológicas De La Universidad De Madrid*, *1*, 189–206.

Canto, C. B., Wouterlood, F. G., & Witter, M. P. (2008). What does the anatomical organization of the entorhinal cortex tell us? *Neural Plasticity*, *2008,* 381243. https://doi.org/10.1155/2008/381243

De Nó, L. (1933). Studies on the structure of the cerebral cortex. I. The area entorhinalis. *Journal of Neurology and Psychology*, *45*, 381–438.

Delbeuck, X., Collette, F., & Linden, M. Van Der. (2007). Is Alzheimer's disease a disconnection syndrome ? Evidence from a crossmodal audio-visual illusory experiment. *Neuropsychologia*, *45*(14), 3315–3323. https://doi.org/10.1016/j.neuropsychologia.2007.05.001

Donato, N. Di, Chiari, S., Mirzaa, G. M., Aldinger, K., Parrini, E., Olds, C., … Dobyns, W. B. (2017). Lissencephaly : Expanded imaging and clinical classification. *American Journal of Medical Genetics*, *173*(6), 1473–1488. https://doi.org/10.1002/ajmg.a.38245

Dunbar, R.I.M., Shultz, S. (2007). Evolution in the Social Brain. *Science*, 317:1344–1347. http://dx.doi.org/10.1126/science.1145463

Fernández, V., Llinares-Benadero, C., & Borrell, V. (2016). Cerebral cortex expansion and folding: what have we learned? *The EMBO Journal, 35*(10), 1021–1044. https://doi.org/10.15252/embj.201593701

Finlay, B.L. (2009). Brain Evolution: Developmental Constraints and Relative Developmental Growth. In: Encyclopedia of Neuroscience. *Elsevier*, 337–345. http://dx.doi.org/10.1016/B978-008045046-9.00939-6

Foubet, O., Trejo, M., & Toro, R. (2019). Mechanical morphogenesis and the development of neocortical organisation. *Cortex, 118*, 315–326. https://doi.org/10.1016/j.cortex.2018.03.005

Fyhn, M., Molden, S., Witter, M. P., Moser, E. I., & Moser, M.-B. (2004). Spatial representation in the entorhinal cortex. *Science (New York, N.Y.)*, *305*(5688), 1258–1264. https://doi.org/10.1126/science.1099901

Gonzales, L. A., Benefit, B. R., Mccrossin, M. L., & Spoor, F. (2015). Cerebral complexity preceded enlarged brain size and reduced olfactory bulbs in Old World monkeys. *Nature Communications*, *6*(7580). https://doi.org/10.1038/ncomms8580

Hadfield, J. (2010). MCMC Methods for Multi-ResponseGeneralized Linear Mixed Models:The MCMCglmm R Package. *Journal of Statistical Software, 33*(2), 1 - 22. https://doi.org/10.18637/jss.v033.i02

Hedges, S., Marin, J., Suleski, M., Paymer, M., & Kumar, S. (2015). Tree of Life Reveals Clock-Like Speciation and Diversification. *Molecular Biology And Evolution, 32(*4), 835-845. doi: 10.1093/molbev/msv037

Hof, P. R., Bouras, C., Perl, D. P., Larry, D., Mehta, N., & Morrison, J. H. (1995). Age-related distribution of neuropathologic changes in the cerebral cortex of patients with Down's syndrome. Quantitative regional analysis and comparison with Alzheimer's disease. *Archives of Neurology*, *52*, 379–391. https://doi.org/10.1001/archneur.1995.00540280065020

Horton, J. C., & Hocking, D. R. (1996). An Adult-Like Pattern of Ocular Dominance Columns in Striate Cortex of Newborn Monkeys prior to Visual Experience. *The Journal of Neuroscience, 16*(5), 1791-1807. https://doi.org/10.1523/JNEUROSCI.16-05-01791.1996

Hyman, B. T., Van Hoesen, G. W., Kromer, L. J., & Damasio, A. R. (1986). Perforant Pathway Changes and the Memory Impairment of Alzheimer's Disease. *Annals of Neurology*, *20*(4), 472–481. https://doi.org/10.1002/ana.410200406

Insausti, R. (1993). Comparative anatomy of the entorhinal cortex and hippocampus in mammals. *Hippocampus*, *3 Spec No*, 19–26. https://doi.org/10.1002/hipo.1993.4500030705

Insausti, R., Herrero, M. T., & Witter, M. P. (1998). Entorhinal cortex of the rat: Cytoarchitectonic subdivisions and the origin and distribution of cortical efferents. Hippocampus, 7(2), 146–183. https://doi.org/10.1002/(sici)1098-1063(1997)7:2<146::aid-hipo4>3.0.co;2-l

Insausti, R., Muñoz-López, M., Insausti, A. M., & Artacho-Pérula, E. (2017). The Human Periallocortex: Layer Pattern in Presubiculum, Parasubiculum and Entorhinal Cortex. A Review. *Frontiers in Neuroanatomy*, *11*, 84. https://doi.org/10.3389/fnana.2017.00084

Jerison, H. J. (1973). Evolution of the Brain and Intelligence. *New York: Academic Press*

Kemper, T. N. (1984). Neuroanatomical and Neuropathological Changes in Normal Aging and in Dementia. *Clinical Neurology of Aging. New York: Oxford University Press*, 9–52.

Kostović, I., Petanjek, Z., & Judas, M. (1993). Early areal differentiation of the human cerebral cortex: entorhinal area. *Hippocampus*, *3*(4), 447–458. https://doi.org/10.1002/hipo.450030406

Kuhn, T., Gullett, J. M., Boutzoukas, A. E., Bohsali, A., Mareci, T. H., FitzGerald, D. B., … Bauer, R. M. (2018). Temporal lobe epilepsy affects spatial organization of entorhinal cortex connectivity. *Epilepsy and Behavior*, *88*, 87–95. https://doi.org/10.1016/j.yebeh.2018.06.038

Kumar, S., Stecher, G., Suleski, M., & Hedges, S. (2017). TimeTree: A Resource for Timelines, Timetrees, and Divergence Times. *Molecular Biology And Evolution, 34*(7), 1812-1819. doi: 10.1093/molbev/msx116

Leontovich, T. A., Mukhina, J. K., Fedorov, A. A., & Belichenko, P. V. (1999). Morphological study of the entorhinal cortex, hippocampal formation, and basal ganglia in Rett syndrome patients. *Neurobiology of Disease*, *6*(2), 77–91. https://doi.org/10.1006/nbdi.1998.0234

Mann, D. M. A., & Esiri, M. M. (1989). The pattern of acquisition of plaques and tangles in the brains of patients under 50 years of age with Down's syndrome. *Journal of the Neurological Sciences*, *89*(2-3), 169–179. https://doi.org/10.1016/0022-510X(89)90019-1

Nieuwenhuys, R.; Voogd, J., van Juijzen, C. (2007). The Human Central Nervous System: Telencephalon: Hippocampus and Related Structures, 4th ed, Berlin. *Springer, 2007*, 361-400.

Pagel, M. (1994). Detecting correlated evolution on phylogenies: a general method for the comparative analysis of discrete characters. (1994). *Proceedings Of The Royal Society Of London. Series B: Biological Sciences, 255*(1342), 37-45. doi: 10.1098/rspb.1994.0006

Paradis, E., & Schliep, K. (2018). ape 5.0: an environment for modern phylogenetics and evolutionary analyses in R. *Bioinformatics, 35*(3), 526-528. https://doi.org/10.1093/bioinformatics/bty633

Perez, S. I., Tejedor, M. F., Novo, N. M., & Aristide, L. (2013). Divergence Times and the Evolutionary Radiation of New World Monkeys (Platyrrhini, Primates): An Analysis of Fossil and Molecular Data. *PLoS ONE, 8*(6), e68029. https://doi.org/10.1371/journal.pone.0068029

Piguet, O., J Chareyron, L., Banta Lavenex, P., G Amaral, D., & Lavenex, P. (2020). Postnatal development of the entorhinal cortex: A stereological study in macaque monkeys. Journal of Comparative Neurology, 528(14), 2308–2332. https://doi.org/10.1002/cne.24897

Revell, L. (2011). phytools: an R package for phylogenetic comparative biology (and other things). *Methods In Ecology And Evolution, 3*(2), 217-223. doi: 10.1111/j.2041-210x.2011.00169.x

Reid, A. T., & Evans, A. C. (2013). Structural networks in Alzheimer's disease. *European Neuropsychopharmacology*, *23*(1), 63–77. https://doi.org/10.1016/j.euroneuro.2012.11.010

Rose, M. (1927). Die sog. Riechrinde beim Menschen und beim Affem. II. Teil des Allocortex bei Tier und Mensch. *Journal of Neurology and Psychology*, *34*, 261–401.

Schmitt, J. E., Raznahan, A., Liu, S., & Neale, M. C. (2020). The Heritability of Cortical Folding: Evidence from the Human Connectome Project. *Cerebral Cortex, 31*(1), 702–715. https://doi.org/10.1093/cercor/bhaa254

Schultz, C., & Engelhardt, M. (2014). Anatomy of the Hippocampal Formation. *Frontiers of Neurology and Neuroscience*, 6–17. https://doi.org/10.1159/000360925

Shultz, S. (2010). Brain Evolution in Vertebrates. *Encyclopedia of Behavioral Neuroscience. Elsevier*, 180–186. http://dx.doi.org/10.1016/B978-0-08-045396-5.00103-2

Solodkin, A., & Van Hoesen, G. W. (1996). Entorhinal cortex modules of the human brain. *Journal of Comparative Neurology*, *365*(4), 610–627. https://doi.org/10.1002/(SICI)1096-9861(19960219)365:4<610::AID-CNE8>3.0.CO;2-7

Stephan, H, Frahm, H., & Baron, G. (1981). New and revised data on volumes of brain structures in insectivores and primates. *Folia Primatologica; International Journal of Primatology*, *35*(1), 1–29. https://doi.org/10.1159/000155963

Stephan, Heinz, & Andy, O. J. (1964). Quantitative Comparisons of Brain Structures from Insectivores to Primates. *American Zoologist*, *4*(1), 59–74. https://doi.org/10.1093/icb/4.1.59

Stephan, Heinz, & Andy, O. J. (1969). Quantitative Comparative Neuroanatomy Of Primates: An Attempt At A Phylogenetic Interpretation. *Annals of the New York Academy of Sciences*, *167*(1), 370–387. https://doi.org/10.1111/j.1749-6632.1969.tb20457.x

Stranahan, A. M., & Mattson M. P. (2010). Selective vulnerability of neurons in layer II of the entorhinal cortex during aging and Alzheimer's disease. *Neural Plast, 2010*, 108190. https://doi.org/10.1155/2010/108190

Van Hoesen, G. W., & Hyman, B. T. (1990). Hippocampal formation : anatomy and the patterns of pathology in Alzheimer's disease. *Progress in Brain Research*, *83*, 445–457. https://doi.org/10.1016/s0079-6123(08)61268-6

Wakabayashi, K., Honer, W. G., & Masliah, E. (1994). Synapse alterations in the hippocampal-entorhinal formation in Alzheimer's disease with and without Lewy body disease. *Brain Research*, *667*(1), 24–32. https://doi.org/10.1016/0006-8993(94)91709-4

White, T., Su, S., Schmidt, M., Kao, C.-Y., & Sapiro, G. (2010). The development of gyrification in childhood and adolescence. *Brain and Cognition*, *72*(1), 36–45. https://doi.org/10.1016/j.bandc.2009.10.009

Woolsey T. A., & Van der Loos, H. (1969). The structural organization of layer IV in the somatosensory region (S1) of mouse cerebral cortex. *Brain Research, 17*, 205-42. https://doi.org/10.1016/0006-8993(70)90079-X

Zilles K, Armstrong E, Moser KH, Schleicher A, S. H. (1989). Gyrification in the cerebral cortex of primates. *Brain Behav Evol.*, 143–150. https://doi.org/10.1159/000116500

Zilles, K., Armstrong, E., Schleicher, A., & Kretschmann, H. (1988). The human pattern of gyrification in the cerebral cortex. *Anatomy and Embryology*, *179*(2), 173-9. https://doi.org/10.1007/bf00304699

Zilles, K., Palomero-Gallagher, N., & Amunts, K. (2013). Development of cortical folding during evolution and ontogeny. *Trends in Neurosciences, 36*(5), 275-84. https://doi.org/10.1016/j.tins.2013.01.006

Figure legends

Figure 1. Entorhinal cortices of 39 primate species. Sections of the entorhinal cortices of 39 species are shown. All images are oriented so that medial is left. Exemplary images from position L3 are shown (most rostral fully medio-laterally extended dentate gyrus visible; explanation in Materials and Methods). Codes refer to Table 1. Scale bars are 0.5 mm on pages 1-4 and 1 mm on page 5. Abbreviations: f = female, m = male.

Figure 2. Hippocampal formation at four selected rostro-caudal positions of exemplary species. Hippocampal formations at positions L1-L4 of seven species are shown (explanation in Materials and Methods, page 7). Codes refer to Table 1. Pages 4-7 are Hominidae. Scale bars are 1 mm. Abbreviations of anatomical structures on page 1: A = amygdala, CA = cornu ammonis, EC = enthorinal cortex, GD = gyrus dentatus, LD = lamina dissecans.

Figure 3. Relationship of cellular island formation with quantitative continuous parameters of primate species. Shown are the relationships of island formation in pre-alpha with the continuous parameters gyrification index (**a**), neopallial volume (**b**), brain weight (**c**), body weight (**d**), neopallial volume-to-brain weight (**e**), and brain weight-to-body weight (**f**). Each data point represents a species (codes refer to Table 1), color indicates assignment to one suborder (Strepsirrhini), one infraorder (Tarsiiformes), and two parvorders (Platyrrhini and Catarrhini). Both *Galagoides demidoff* individuals (S14 and S15) were excluded in statistical calculations. Abbreviations: b = between - pre-alpha is wavy or partly discontinuous; n = no islands; y = yes - islands visible.

Figure 4. Ancestral character state reconstruction of cellular island formation in the primate lineage. Pie charts provide the likelihood that an ancestor exhibited a particular characteristic in pre-alpha by taking into account the relatedness of all species and the cellular island categories of all species included. Both *Galagoides demidoff* individuals (S14 and S15) were excluded in statistical calculations as their different island traits would influence the likelihoods of their ancestral states. Colors of the linkage lines refer to the colors for the primate groups in Figure 3. Species codes refer to Table 1. Abbreviations: b = between – pre-alpha is wavy or partly discontinuous; n = no islands; y = yes – islands visible.

Figure 5. Human lissencephalies lack pre-alpha islands. A coronal section of a human lissencephalic mediobasal temporal cortex is provided (case 1; **(a)**). The left image shows the brain of an 8-year-old male with the Ammon's horn (CA), subiculum (SUB), and entorhinal cortex (EC). At right, a magnification of the highlighted area in the left image is depicted (**b**). The layers are highlighted from deep to superficial layers as stratum principale internum (SPI), stratum principale externum (SPE), and the lamina dissecans (LD) separating them. Pre-alpha stands for pre-alpha layer and shows no cellular islands in this case. The full dorso-ventral extent of EC of a 13-year-old female individual is depicted in **(c)** (case 2). The latter harbors no islands. The EC of a 15-year-old female control with no brain abnormalities and a clearly visible pre-alpha layer with islands is shown for comparison **(d)**. Arrows highlight islands.

Graphical abstract. The drawing at the top show coronal sections through a gyrified human brain (at left) and a lissencephalic ('smooth', i.e., lacking normal convolutions) human brain (at right). The lower half of the image shows exemplary images of primate brains with a strongly gyrified cortex (*Pongo pygmaeus*) versus a comparatively smooth brain surface (*Perodicticus potto*). Whereas the pre-alpha layer in *Pongo pygmaeus* (at left) displays cellular islands, these

are lacking in the lissencephalic primate (at right). The images are identical to those shown in Figure 1.

Supplementary figure. Entorhinal cortex of a newborn. A coronal section of a 1-day-old male is provided. Abbreviations: EC = entorhinal cortex, LD = lamina dissecans, SPE = stratum principale externum, SPI = stratum principale internum.

Table 1. Overview of data from 39 primates. Continuous species parameters are taken from Zilles et al. (1989). Abbreviations: b = between – pre-alpha is wavy or partly discontinuous; GI = gyrification index; IF = island formation (final value); n = no islands; NA = not available; NEO = neopallium volume; L1, L2, L3, L4 = four positions of cellular island formation from rostral to caudal; y = yes – islands visible.

Table 2. Demographic and neuropathological data for the three human cases studied. Cases 1 and 2 are from lissencephalic individuals; case 3 is a control case. Fresh brain weight in grams. The information in additional data and neurological histopathology were extracted from documents of the NIH Neurobiobank. Abbreviations: f = female, m = male; age (in years).

Figure 1, page 1

Strepsirrhini

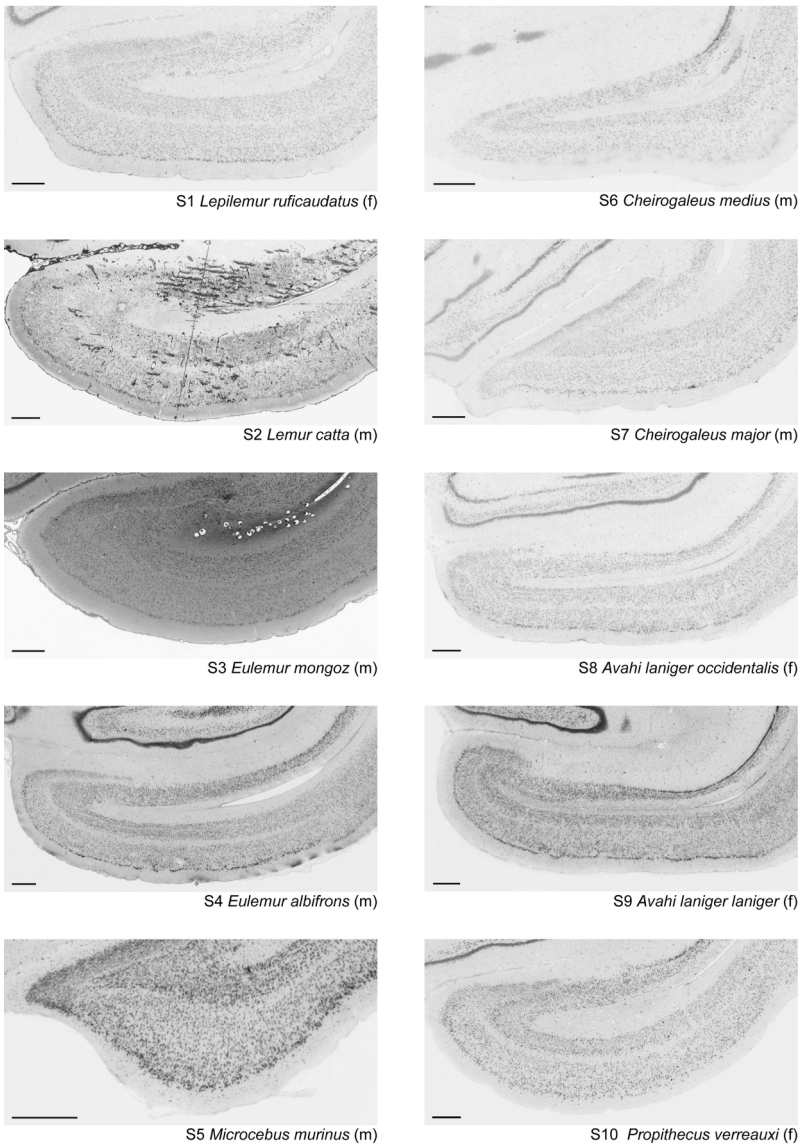

CNE_25233_Figure 1 part1.tif

Figure 1, page 2

Strepsirrhini

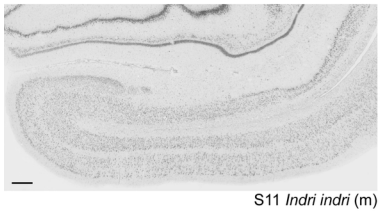

S11 *Indri indri* (m)

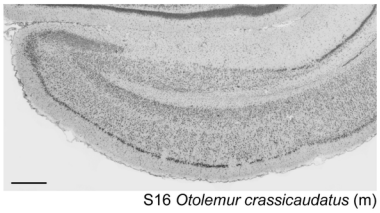

S16 *Otolemur crassicaudatus* (m)

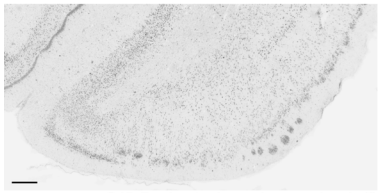

S12 *Daubentonia madagascariensis* (f)

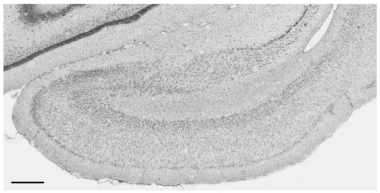

S17 *Nycticebus cougang* (f)

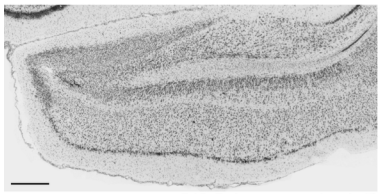

S13 *Galago senegalensis* (f)

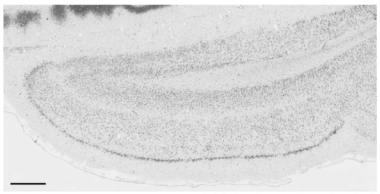

S18 *Loris tardigradus* (m)

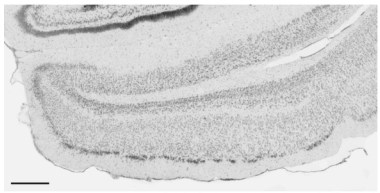

S14 *Galagoides demidoff*/a (m)

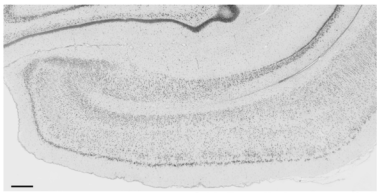

S19 *Perodicticus potto* (m)

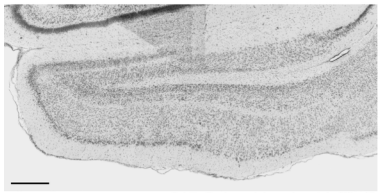

S15 *Galagoides demidoff*/b (f)

CNE_25233_Figure 1 part2.tif

Figure 1, page 3

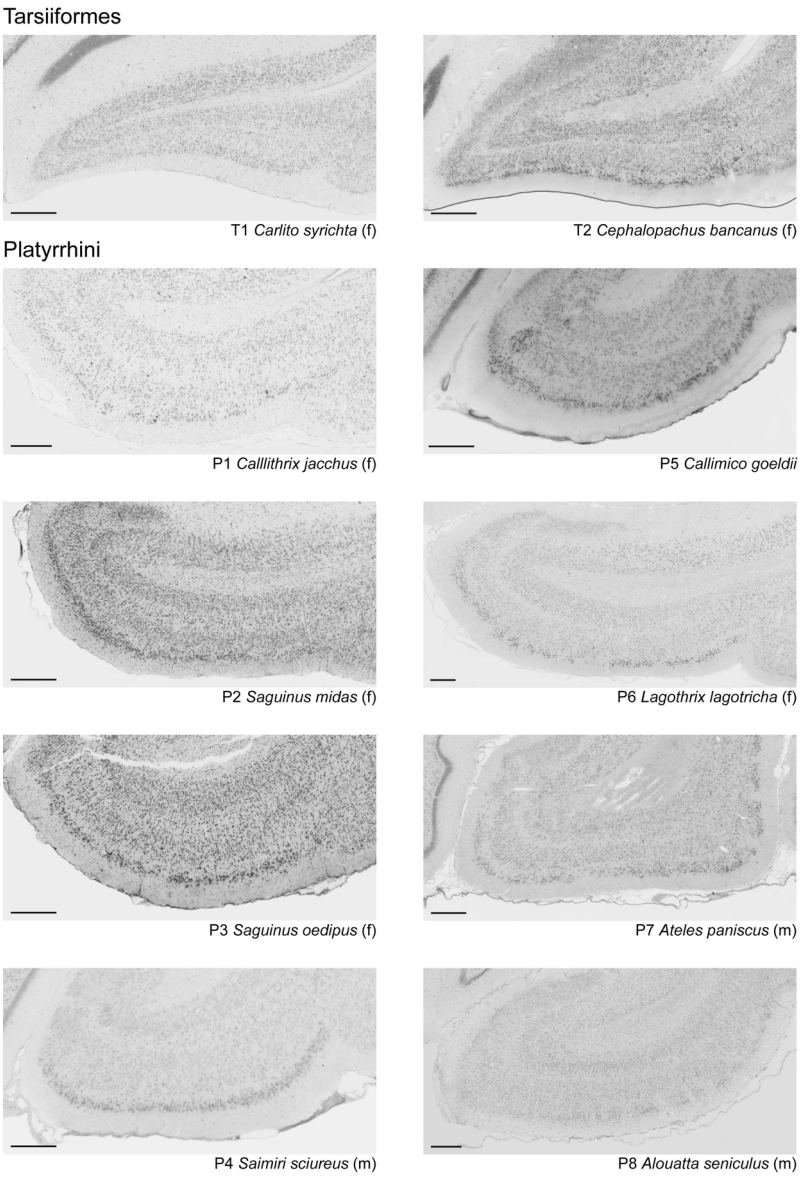

CNE_25233_Figure 1 part3.tif

Figure 1, page 4

Catarrhini: Cercopithecoidea

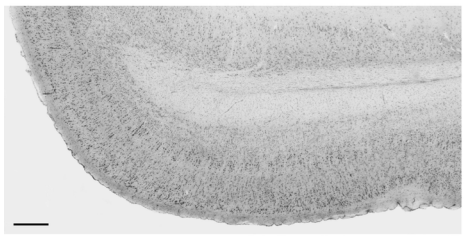

C1 *Pygathrix nemaeus* (f)

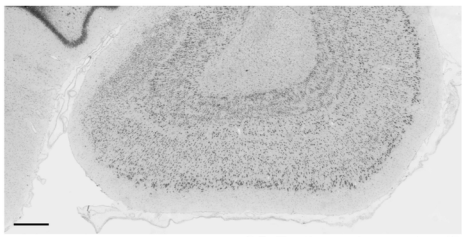

C5 *Erythrocebus patas* (f)

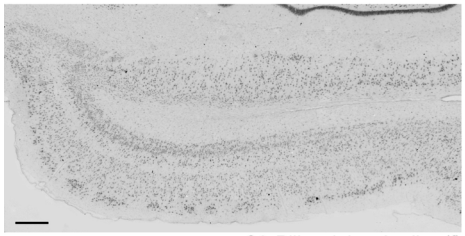

C2 *Piliocolobus badius* (f)

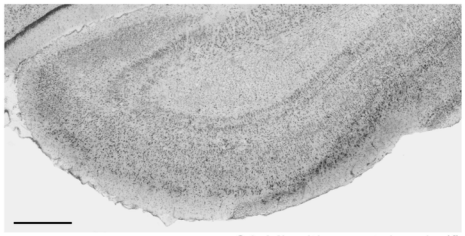

C6 *Miopithecus talapoin* (f)

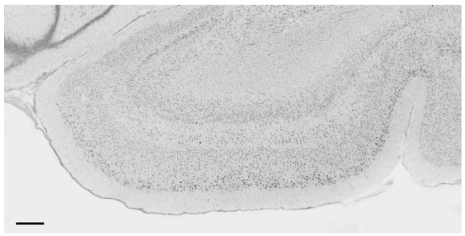

C3 *Lophocebus albigena* (f)

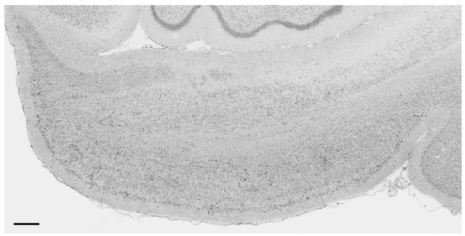

C7 *Hylobates lar* (m)

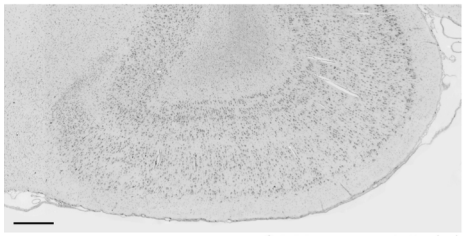

C4 *Macaca mulatta* (m)

CNE_25233_Figure 1 part4.tif

Figure 1, page 5

Catarrhini: Hominidae

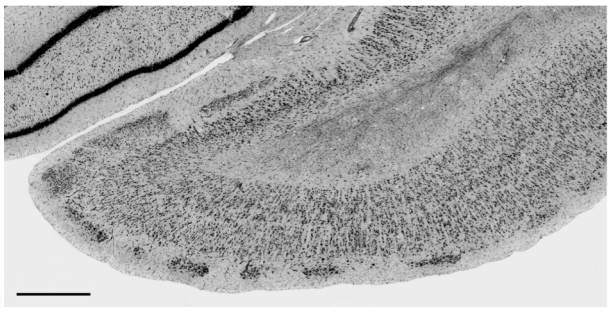

C8 *Pongo pygmaeus* (m)

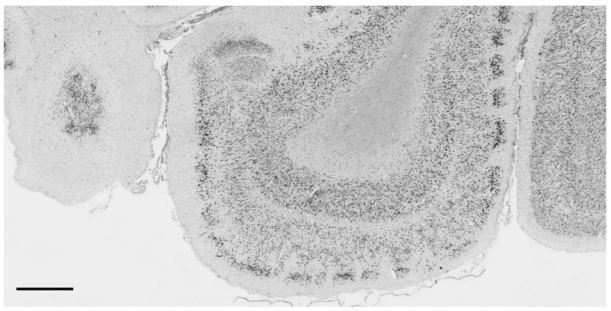

C10 *Gorilla gorilla* (f)

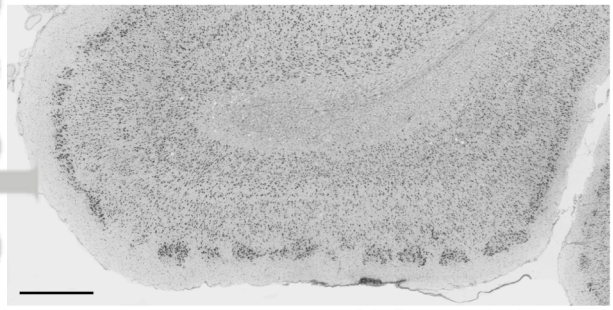

C9 *Pan troglodytes* (m)

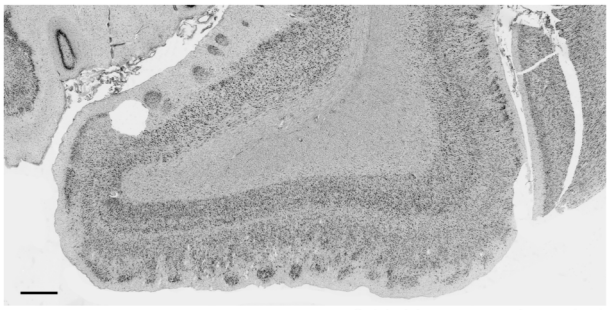

C11 *Homo sapiens* (m)

CNE_25233_Figure 1 part5.tif

Figure 2, page 1

S4 *Eulemur albifrons*

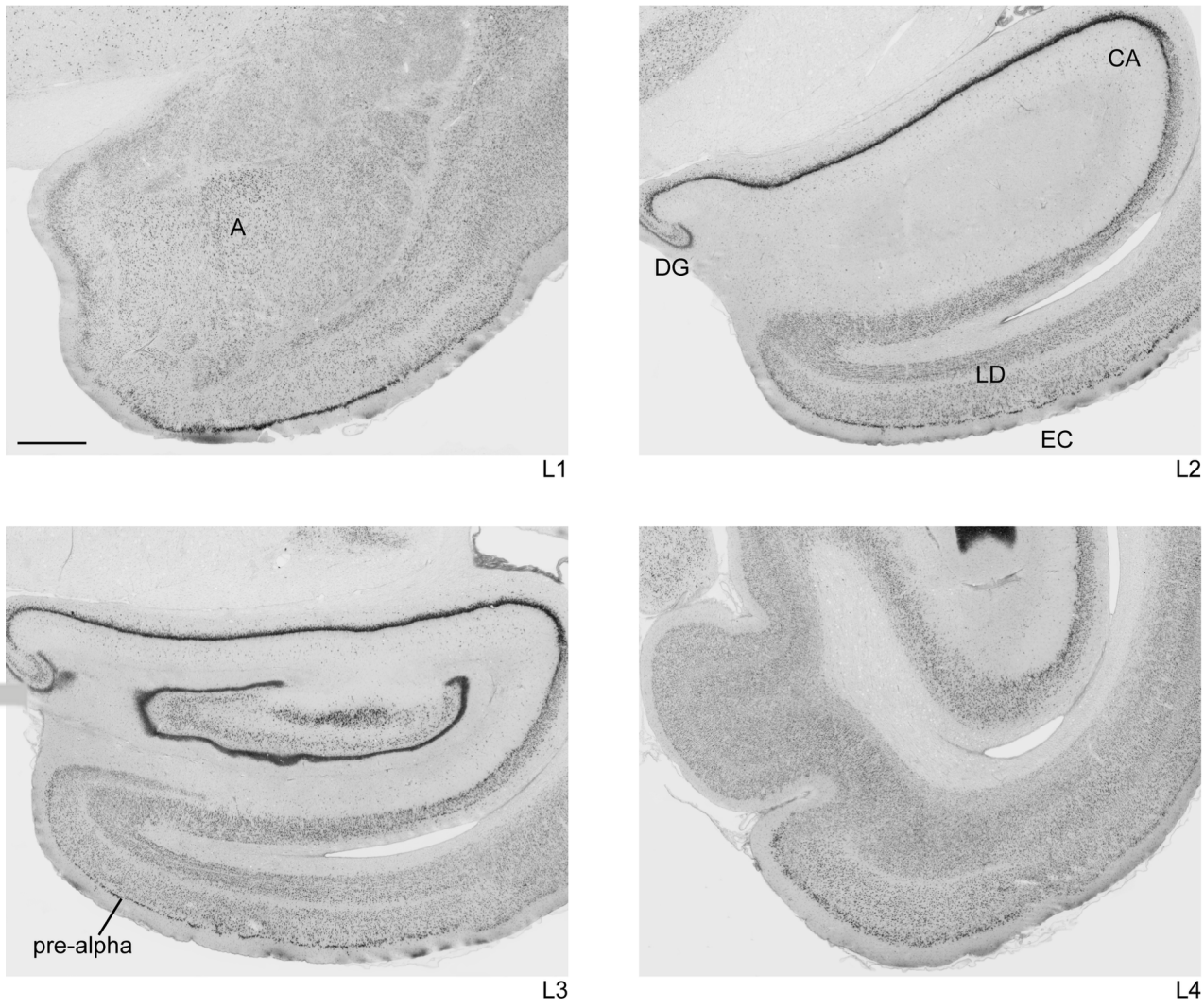

CNE_25233_Figure 2 part1.tif

Figure 2, page 2

S19 *Perodicticus potto*

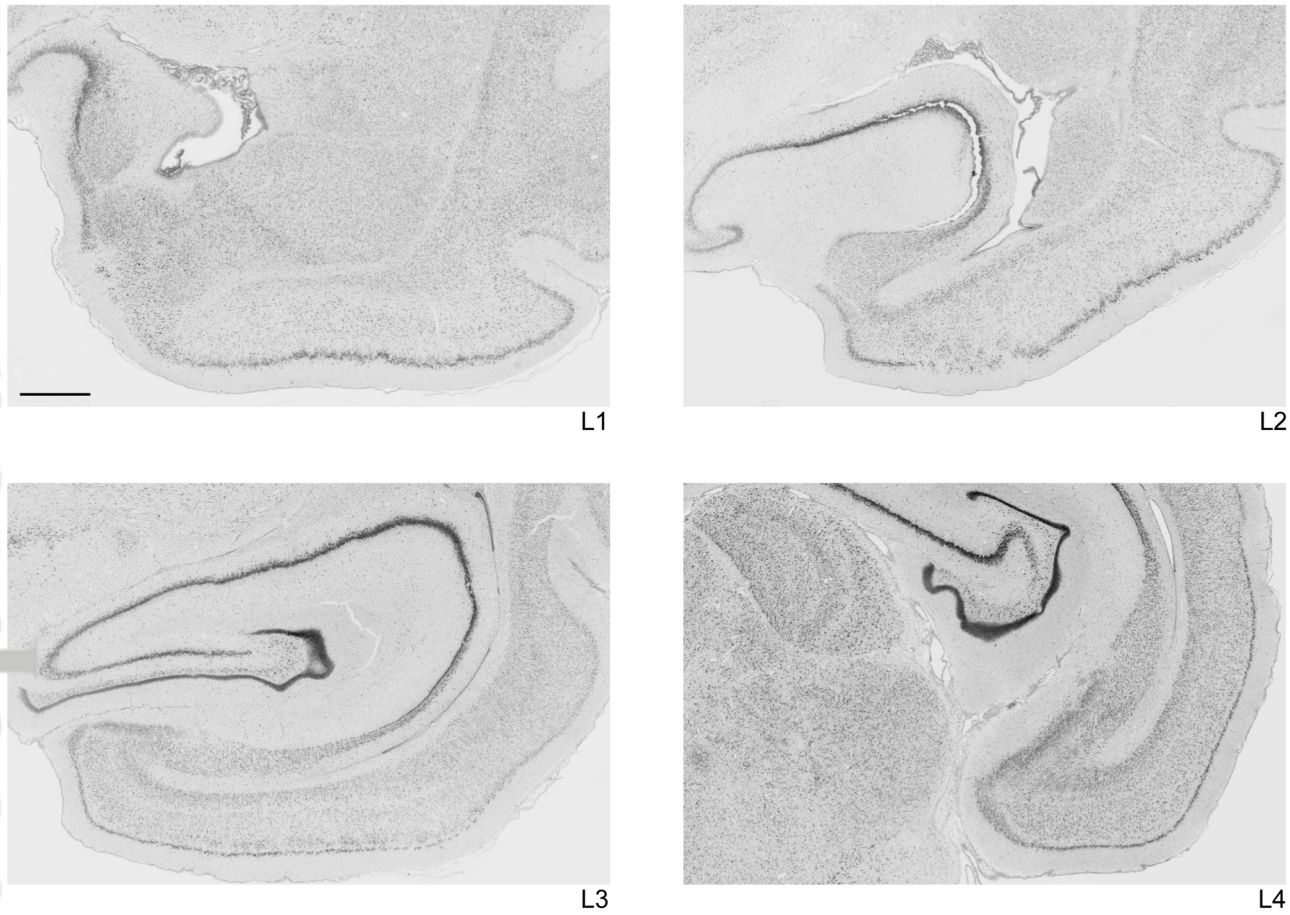

CNE_25233_Figure 2 part2.tif

Figure 2, page 3

P7 *Ateles paniscus*

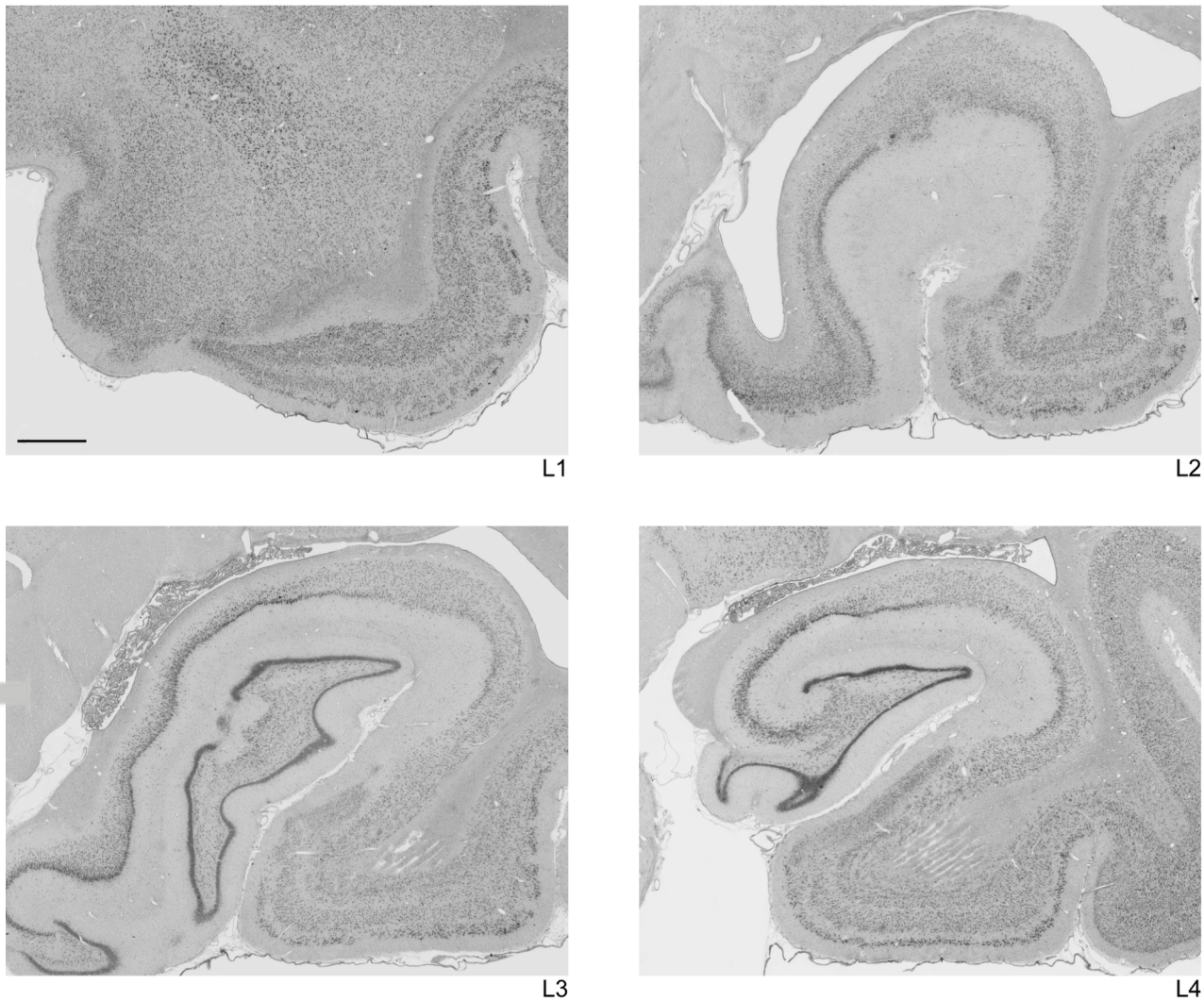

CNE_25233_Figure 2 part3.tif

Figure 2, page 4

C8 *Pongo pygmaeus*

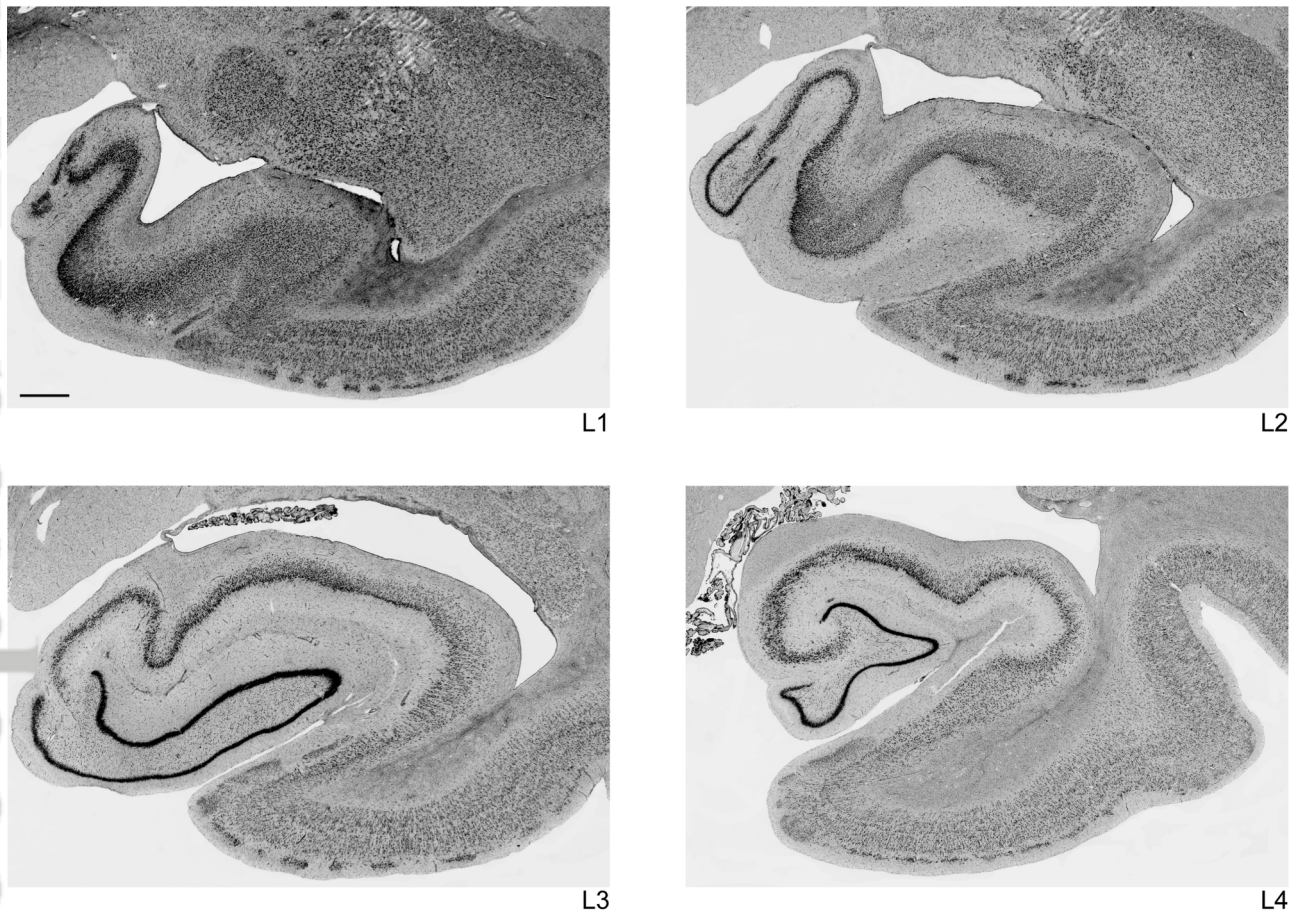

CNE_25233_Figure 2 part4.tif

Figure 2, page 5

C9 *Pan troglodytes*

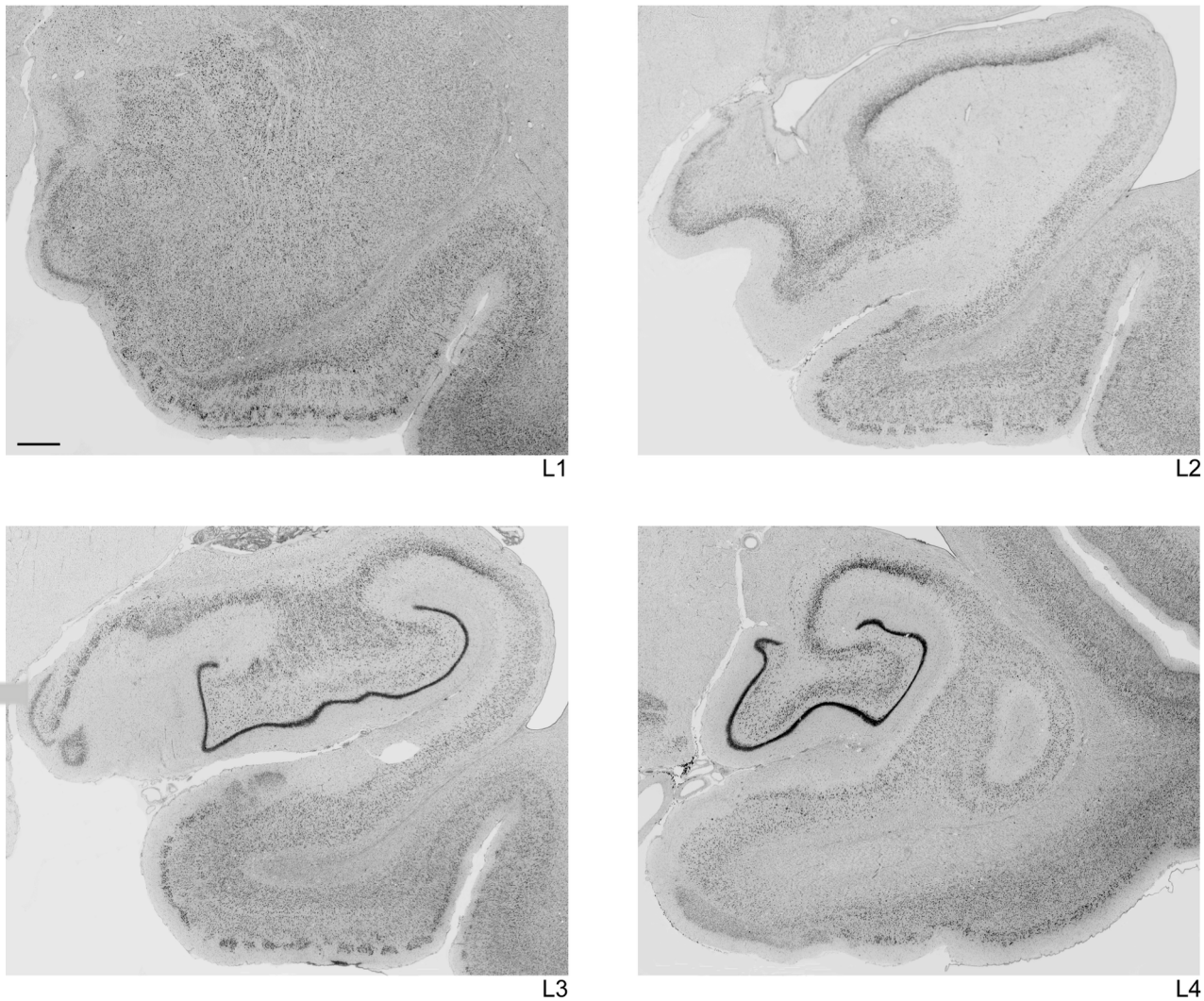

CNE_25233_Figure 2 part5.tif

Figure 2, page 6

C10 *Gorilla gorilla*

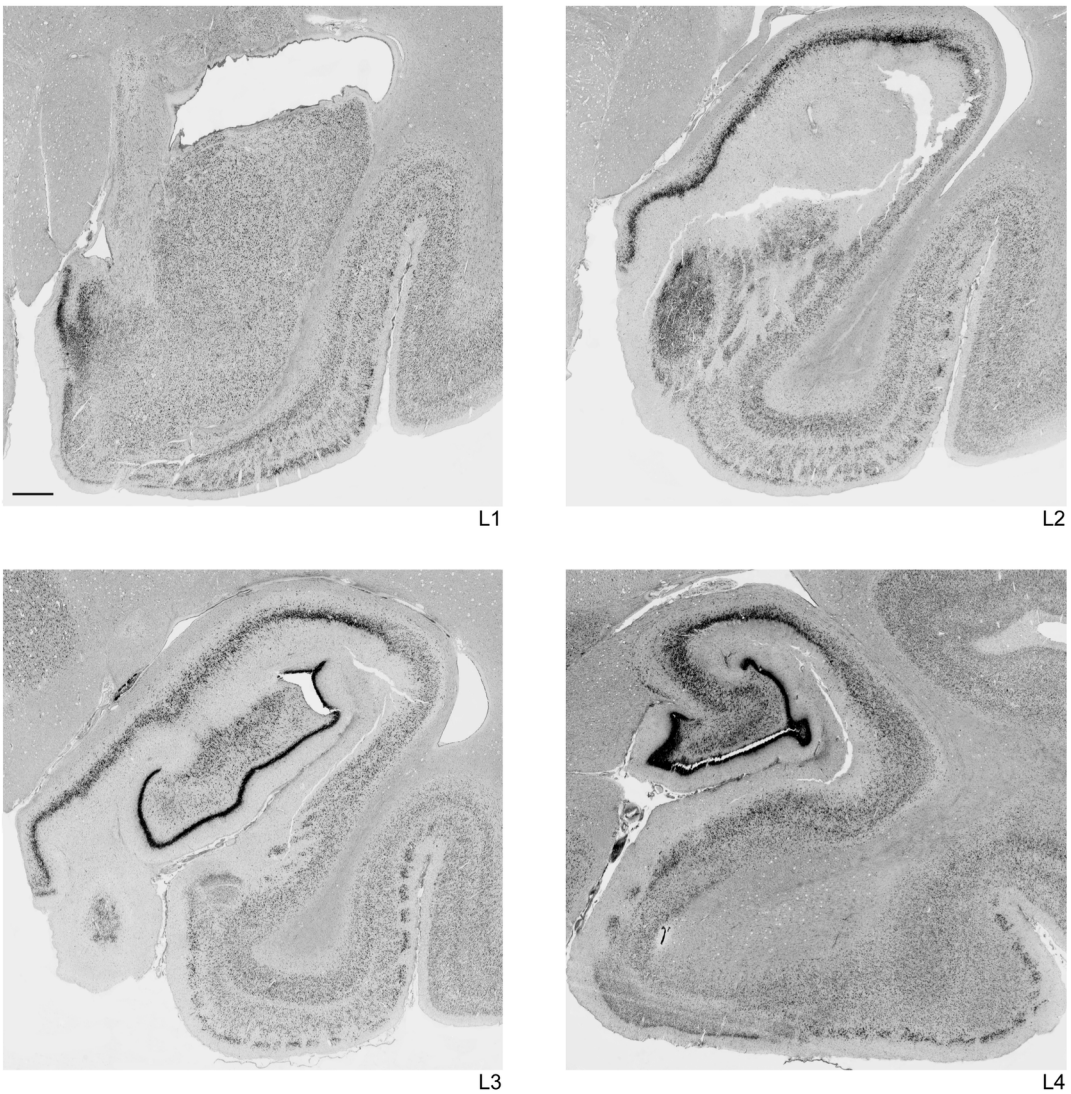

CNE_25233_Figure 2 part6.tif

Figure 2, page 7

C11 *Homo sapiens*

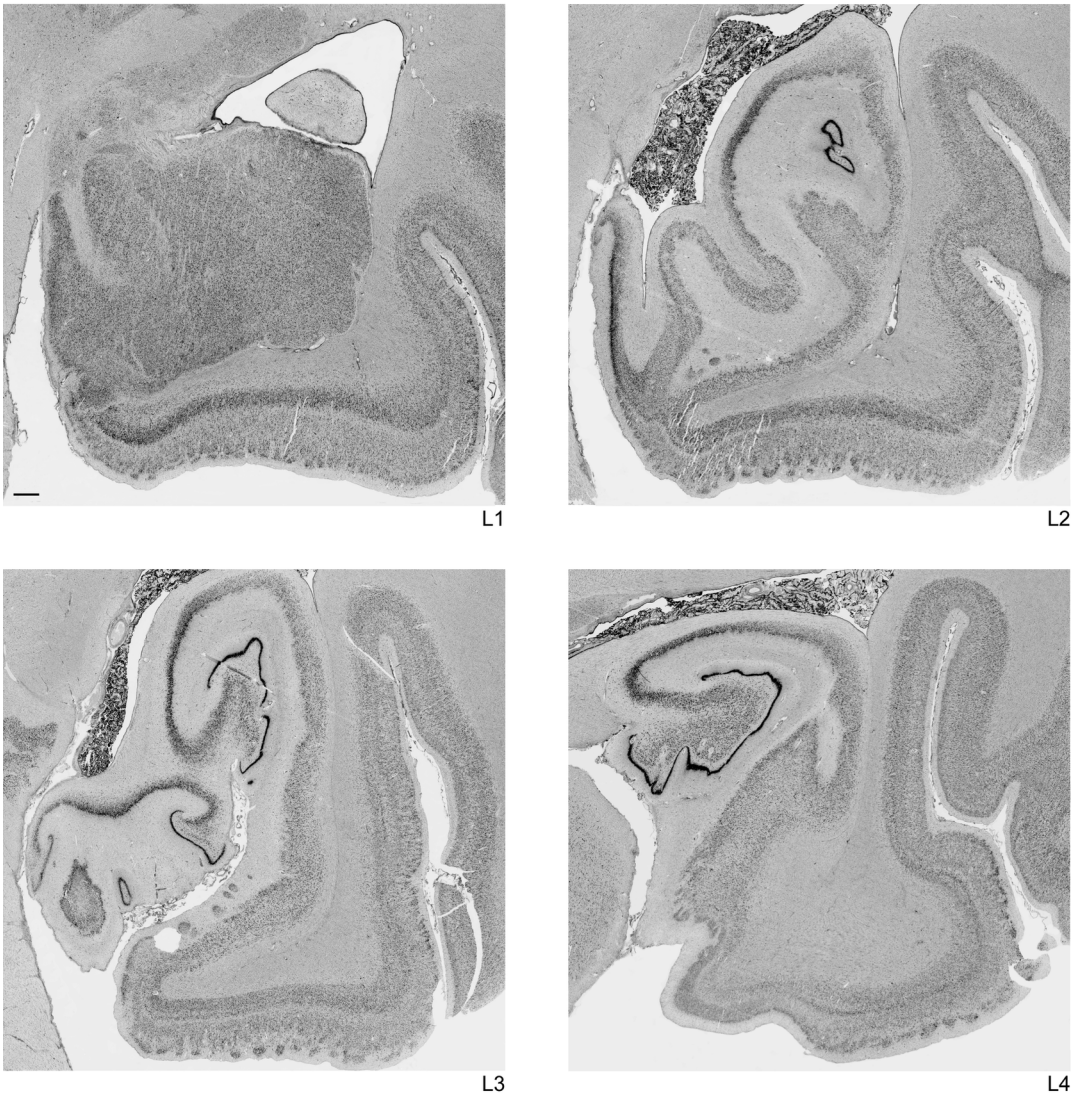

CNE_25233_Figure 2 part7.tif

Figure 3, page 1

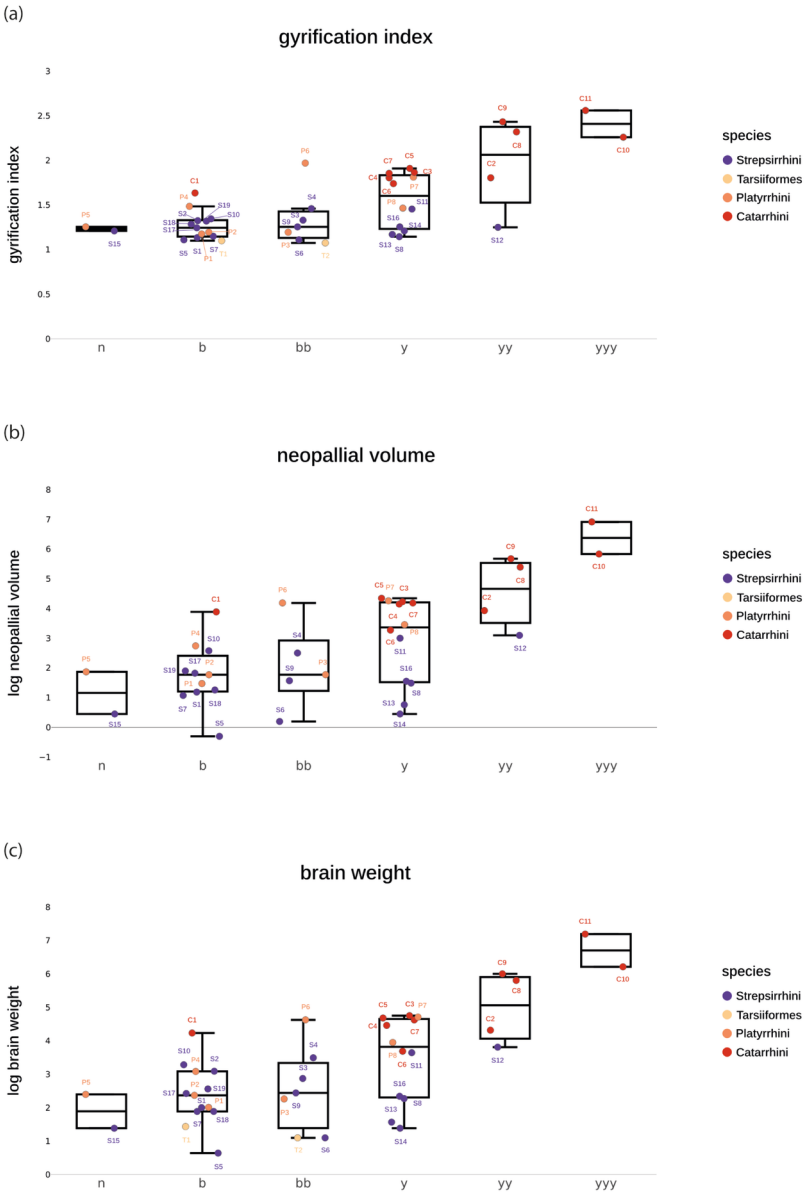

CNE_25233_Figure 3 part1.tif

Figure 3, page 2

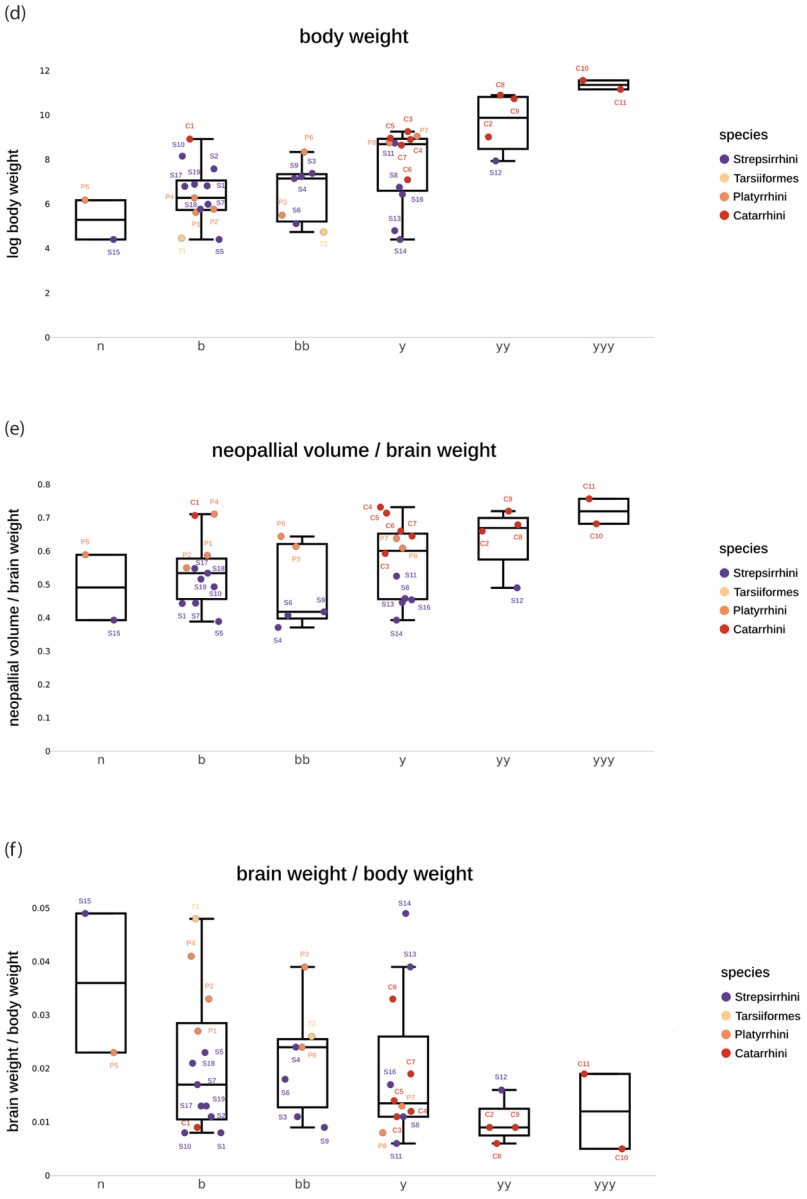

CNE_25233_Figure 3 part2.tif

Figure 4

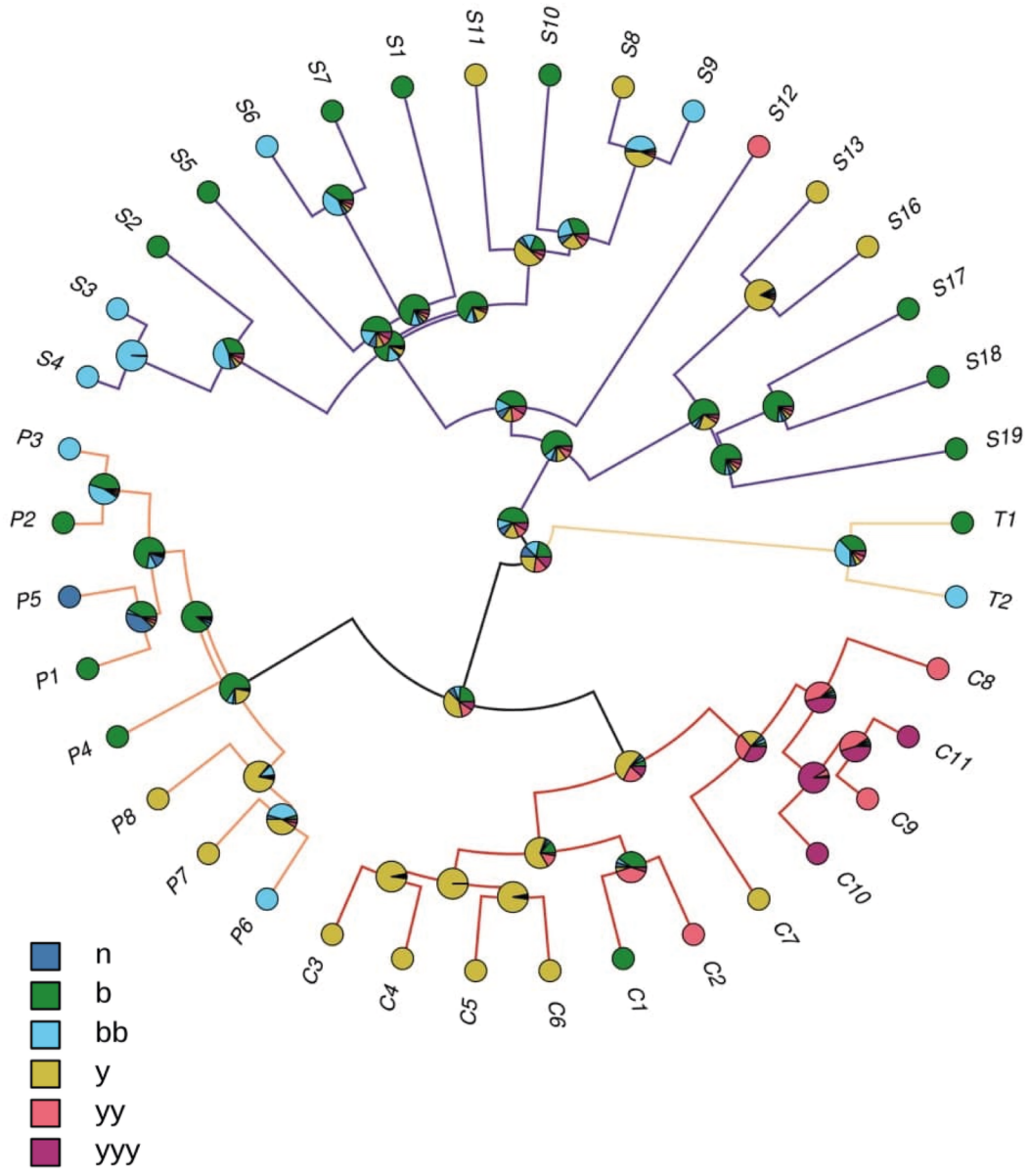

CNE_25233_Figure 4.tif

Figure 5

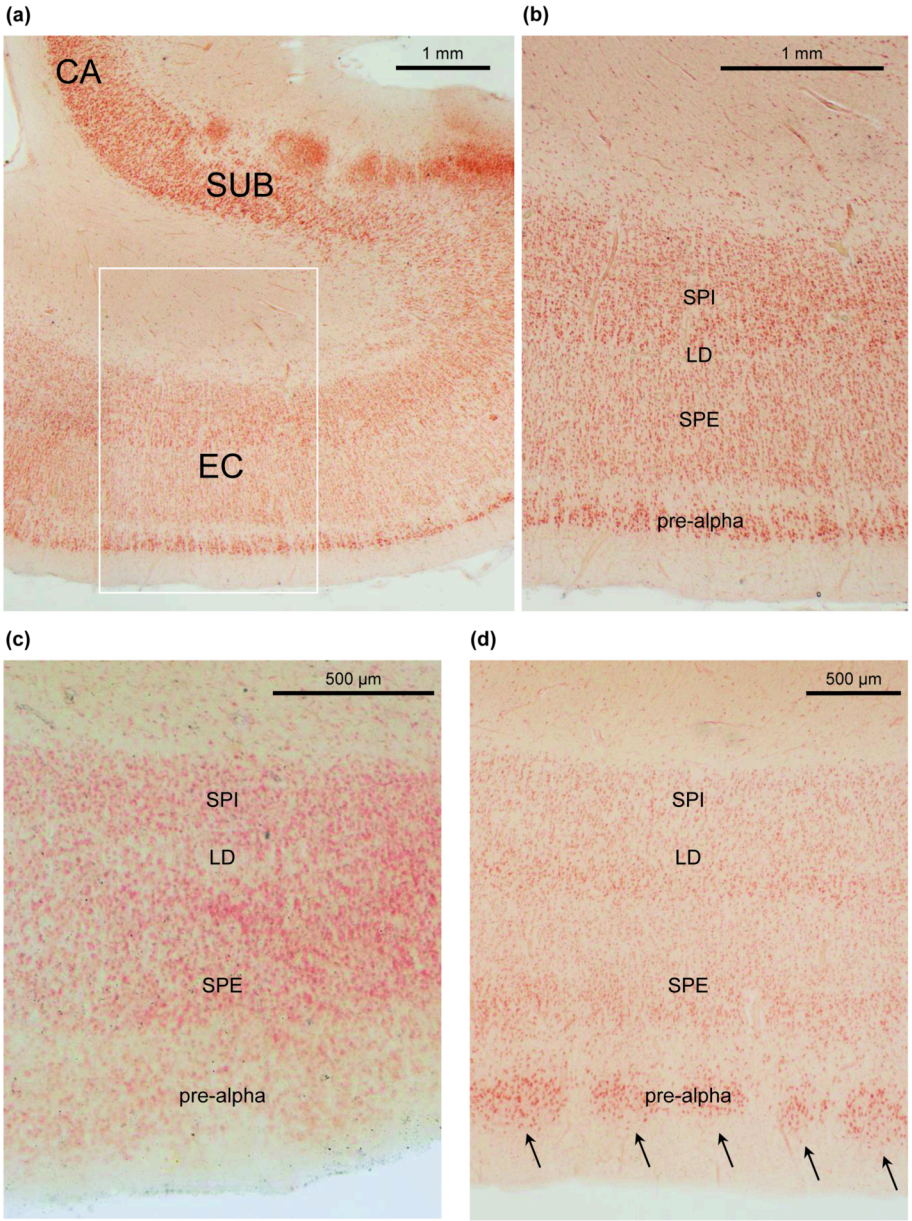

CNE_25233_Figure 5.tif

Graphical abstract. The drawing at the top show coronal sections through a gyrified human brain (at left) and a lissencephalic ('smooth', i.e., lacking normal convolutions) human brain (at right). The lower half of the image shows exemplary images of primate brains with a strongly gyrified cortex (*Pongo pygmaeus*) versus a comparatively smooth brain surface (*Perodicticus potto*). Whereas the pre-alpha layer in *Pongo pygmaeus* (at left) displays cellular islands, these are lacking in the lissencephalic primate (at right). The images are identical to those shown in Figure 1.

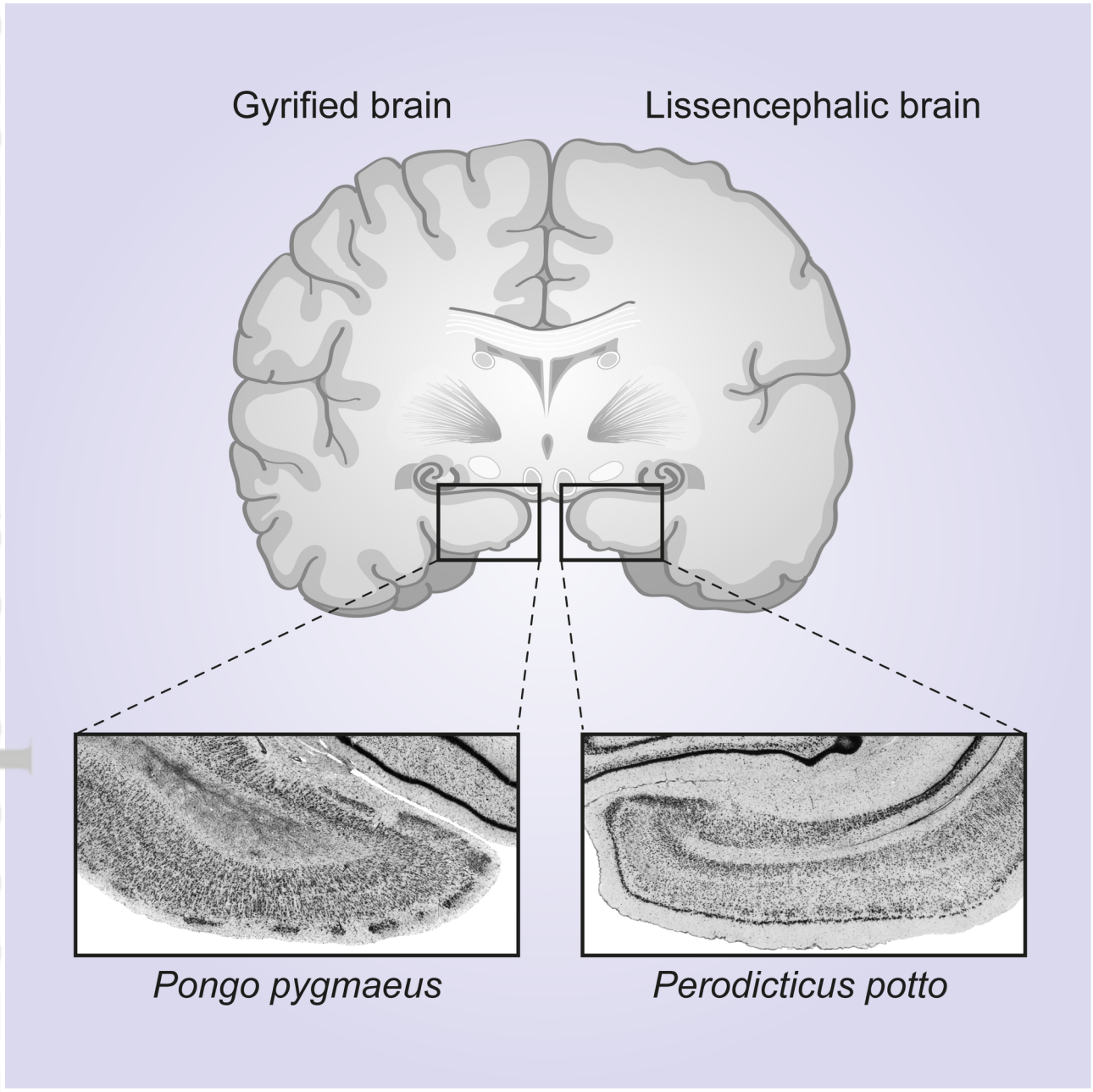

CNE_25233_Graphical abstract.tif

Supplementary figure

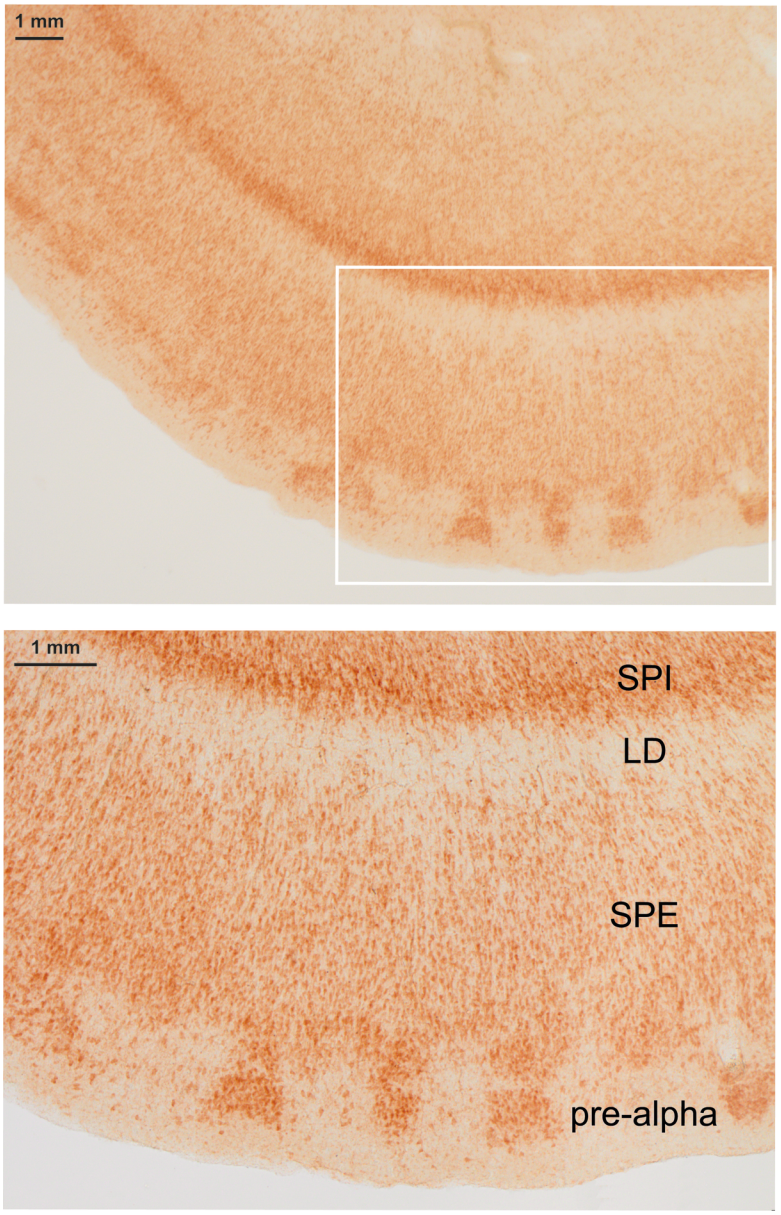

CNE_25233_Supplementary figure.tif

Table 1

ID	Species	body weight (g)	brain weight (g)	NEO (cm^3)	NEO / brain Weight	brain weight / body weight	GI	L 1	L 2	L 3	L 4	IF
	Strepsirrhini											
S1	*Lepilemur ruficaudatus*	915	7.4	3.28	0.443	0.008	1.135	b	b	n	n	b
S2	*Lemur catta*	1960	22	NA	NA	0.011	1.325	b	n	n	n	b
S3	*Eulemur mongoz*	1600	17.7	NA	NA	0.011	1.33	n	b	b	n	bb
S4	*Eulemur albifrons*	1385	32.9	12.21	0.371	0.024	1.46	n	b	b	n	bb
S5	*Microcebus murinus*	82	1.9	0.74	0.389	0.023	1.11	b	b	n	n	b
S6	*Cheirogaleus medius*	167	3	1.22	0.407	0.018	1.11	b	b	b	n	bb
S7	*Cheirogaleus major*	400	6.6	2.93	0.444	0.017	1.15	b	b	n	n	b
S8	*Avahi laniger occidentalis*	860	9.7	4.44	0.458	0.011	1.145	y	b	n	n	y
S9	*Avahi laniger laniger*	1270	11.5	4.81	0.418	0.009	1.255	b	b	b	n	bb
S10	*Propithecus verreauxi*	3480	26.7	13.17	0.493	0.008	1.345	b	n	n	n	b
S11	*Indri indri*	6250	38.3	20.11	0.525	0.006	1.455	y	b	n	n	y
S12	*Daubentonia madagascariensis*	2800	45.2	22.13	0.49	0.016	1.25	b	y	y	b	yy
S13	*Galago senegalensis*	122	4.8	2.14	0.446	0.039	1.17	b	y	n	n	y
S14	*Galagoides demidoff* a	82	4	1.57	0.393	0.049	1.21	b	b	y	n	y
S15	*Galagoides demidoff* b	82	4	1.57	0.393	0.049	1.21	n	n	n	n	n

ID	Species	body weight (g)	brain weight (g)	NEO (cm^3)	NEO / brain weight	brain weight / body weight	GI	L 1	L 2	L 3	L 4	IF
S16	*Otolemur crassicaudatus*	625	10.4	4.72	0.454	0.017	1.255	y	y	b	n	y
S17	*Nycticebus coucang*	895	11.3	6.19	0.548	0.013	1.245	b	b	n	n	b
S18	*Loris tardigradus*	322	6.6	3.52	0.534	0.021	1.285	b	n	n	n	b
S19	*Perodicticus potto*	980	12.95	6.68	0.516	0.013	1.32	n	b	n	n	b
	Haplorhini (Tarsiiformes)											
T1	*Carlito syrichta*	87	4.2	NA	NA	0.048	1.1	b	n	n	n	b
T2	*Tarsius bancanus*	115	3	NA	NA	0.026	1.075	b	b	b	n	bb
	Haplorhini (Semiformes/Platyrrhini)											
P1	*Callithrix jacchus*	277.5	7.45	4.37	0.587	0.027	1.176	b	b	n	n	b
P2	*Saguinus midas*	320	10.7	5.88	0.55	0.033	1.195	n	n	n	b	b
P3	*Saguinus oedipus*	244	9.6	5.89	0.614	0.039	1.195	b	b	b	b	bb
P4	*Saimiri sciureus*	532.5	21.85	15.54	0.711	0.041	1.485	b	n	n	n	b
P5	*Callimico goeldii*	480	11	6.48	0.589	0.023	1.255	n	n	n	n	n
P6	*Lagothrix lagotricha*	4190	102.3	65.87	0.644	0.024	1.97	b	b	b	n	bb
P7	*Ateles paniscus*	8500	111	70.86	0.638	0.013	1.813	y	y	b	n	y
P8	*Alouatta seniculus*	6400	52	31.66	0.609	0.008	1.465	y	y	b	n	y

ID	Species	body weight (g)	brain weight (g)	NEO (cm^3)	NEO / brain Weight	brain weight / body weight	GI	L 1	L 2	L 3	L 4	IF
	Haplorhini (Semiformes/Catarrhini)											
C1	*Pygathrix nemaeus*	7500	69	48.76	0.707	0.009	1.635	b	n	n	n	b
C2	*Piliocolobus badius*	8250	75	50.91	0.679	0.009	1.805	y	y	y	b	yy
C3	*Lophocebus albigena*	10500	116	68.73	0.593	0.011	1.865	y	b	n	n	y
C4	*Macaca mulatta*	7350	86.7	63.48	0.732	0.012	1.805	y	n	n	n	y
C5	*Erythrocebus patas*	7800	108	77.14	0.714	0.014	1.91	y	b	n	n	y
C6	*Miopithecus talapoin*	1200	40	26.43	0.66	0.033	1.74	y	b	b	n	y
C7	*Hylobates lar*	5700	102	65.8	0.645	0.019	1.855	y	b	n	n	y
	Haplorhini: Hominidae (Semiformes/Catarrhini)											
C8	*Pongo pygmaeus*	54000	333	219.8	0.66	0.006	2.32	b	y	y	y	yy
C9	*Pan troglodytes*	46000	405	291.59	0.72	0.009	2.433	y	y	y	n	yy
C10	*Gorilla gorilla*	105000	500	341.44	0.682	0.005	2.26	y	y	y	y	yyy
C11	*Homo sapiens*	70000	1330	1006.5	0.757	0.019	2.56	y	y	y	y	yyy

Table 2

case	age	f/m	hemisphere	fresh brain weight	additional data	neurological histopathology
lissencephaly						
1	8	f	right	620	Unknown lissencephaly syndrome; blindness (bilateral colobomas), bilateral hearing loss, severe scoliosis, as a newborn difficult feeding (dysphagia), muscular hypotonia, pneumonia. Craniofacial abnormalities and other dysmorphic changes. Severely delayed development: inability to sit, crawl, stand, walk, or speak. Some vocalization. MRI: smooth surface; thickened cortex.	Lissencephaly with features of pachygyria; only inferior frontal sulci and major fissures present; cortical ribbon markedly thickened with a white line separating an outer from an inner layer; thinning of the corpus callosum; indistinct separation of the caudate nucleus from putamen; benign parenchymal cyst of the left cerebellum.
2	13	m	right	1056	Minor facial dysmorphism. Develop-mentally disabled. Genetics: deletion in the lissencephaly critical region of chromosome 17: LIS-1 (Miller-Dieker) microdeletion; MRI: moderate or grade 3 lissencephaly with pachygyria over frontal lobe to sylvian region; beyond that point agyria; small remnant of corpus callosum.	Type 1 lissencephaly; cortex with smooth pattern with minimal sulcation; thick four-layered cerebral cortex in the retro-sylvian cerebrum; hypoplastic hippocampus; hypoplastic degenerating cerebellum, ; heterotopic remnants of inferior olive in the mid-medulla oblongata.
control						
3	15	f	left	1450	Malignom (ovary) with extensive peritoneal carcinomatosis.	Normal cortical morphology. No intracranial metastases.